DOTTORATO DI RICERCA IN
BASIC AND APPLIED BIOMEDICAL SCIENCES
(XXXII CICLO)

Coordinatore:

Prof.ssa Stefania Stefani

NOVEL STRATEGIES TO OVERCOME BORTEZOMIB RESISTANCE IN MULTIPLE MYELOMA

Dottorando

Dott.ssa Giuseppina Camiolo

Tutor: Chiar. mo Prof. Roberto Avola

Co-tutor: Prof. Daniele Tibullo

ANNO ACCADEMICO

2018-2019

Indice

Background

1. Multiple Myeloma

1.1 Pathophysiology

Multiple myeloma is a hematological malignancy of differentiated plasma cells and is the second most common haematological malignancy after non-Hodgkin lymphoma [1]. In most patients, multiple myeloma is characterized by the secretion of monoclonal immunoglobulin proteins (known as M protein or monoclonal protein), which are produced by the abnormal plasma cells [2];[3]. The clinical manifestations of disease are driven by the malignant cells or cytokines secreted by the malignant cells, and include signs of organ damage, such as hypercalcaemia, renal insufficiency, anaemia, and/or bone disease with lytic lesions (that is, lesions caused by a disease process) or pathological fractures, which are collectively known as CRAB features [4]. Multiple Myeloma (MM) encompasses a spectrum of clinical variants ranging from benign Monoclonal Gammopathies of Undetermined Significance (MGUS) and smoldering/indolent MM, to more aggressive, disseminated forms of MM and PC leukemia. Within these disorders, the most common is monoclonal gammopathy of undetermined significance (MGUS), characterized by the infiltration of clonal plasma cells into the bone marrow and the secretion of monoclonal protein. MGUS is asymptomatic and precedes the development of multiple myeloma, with or without an identified intervening stage, referred to as smouldering multiple myeloma (SMM) [fig.1] [5], [6]. Multiple myeloma is a biologically heterogeneous disease. Insight into B cell development and plasma cell biology is essential for understanding multiple myeloma. Plasma cells develop from haematopoietic stem cells, which undergo several rounds of differentiation in the bone marrow and secondary lymphoid organs to B cells and eventually to plasma cells. In the bone marrow, immature B cells undergo V(D)J rearrangement, a process that generates their diverse primary immunoglobulin repertoire [7]. B cells with a IgH–IgL complex (B cell receptor) on cell surface migrate to secondary lymphoid organs, such as the lymph node or the spleen. In these secondary lymphoid organs, B cells undergo several processes (affinity maturation, somatic hypermutation and class-switch recombination) that result in the production of antibodies which have a high affinity for specific antigens and with different functional properties. Double-strand DNA breaks in the immunoglobulin loci are needed for recombinations and somatic hypermutations.

However, these DNA breaks can fuse with other breaks that occur in the genome, leading to aberrant fusions of DNA and chromosomal translocations. However, translocations involving specific oncogenes can give cells a growth advantage, which could lead to the development of pathological states, such as MGUS, SMM and eventually multiple myeloma. Thus, chromosomal translocations are a possible initiating event for a subset of multiple myeloma cases. Models of multiple myeloma development have contributed to our understanding of this disease [8], [9]. Translocation t(11;14), which is found in 14% of all patients with multiple myeloma, results in increased expression of CCND1, whose product, cyclin D1, is important for cell cycle progression. Other chromosomal defects observed in patients with multiple myeloma include loss of the short arm of chromosome 1 (del(1p)), gain of the long arm of chromosome 1 (gain(1q)), deletion of the long arm of chromosome 13 (del(13q)) and loss of the short arm of chromosome 17 (del(17p) [10], [11]. Epigenetic defects studied in multiple myeloma include altered DNA methylation, chromatin structure and miRNA deregulation. Levels of hypermethylation are similar in MGUS and multiple myeloma, whereas levels of hypomethylation are increased in multiple myeloma, suggesting that this might play a role in disease development [12], [13]. Several miRNAs are present at different levels in multiple myeloma cells, when compared to normal plasma cells, or MGUS cells, including upregulation of miR-19a and miR-19b in multiple myeloma [14]. miR-19a and miR-19b can contribute to Janus kinase–signal transducer and activator of transcription (JAK–STAT) pathway activation through targeting the JAK–STAT inhibitor suppressor of cytokine signalling 1 (SOCS1). JAK–STAT signalling is important in multiple myeloma for regulating sensitivity to cytokines, and consequentially survival [14]. In addition, reduced levels of miR-30-5p could be associated with increased levels of B cell CLL/lymphoma 9 protein (BCL9; a transcriptional co- activator of WNT–β-catenin signalling) [15].

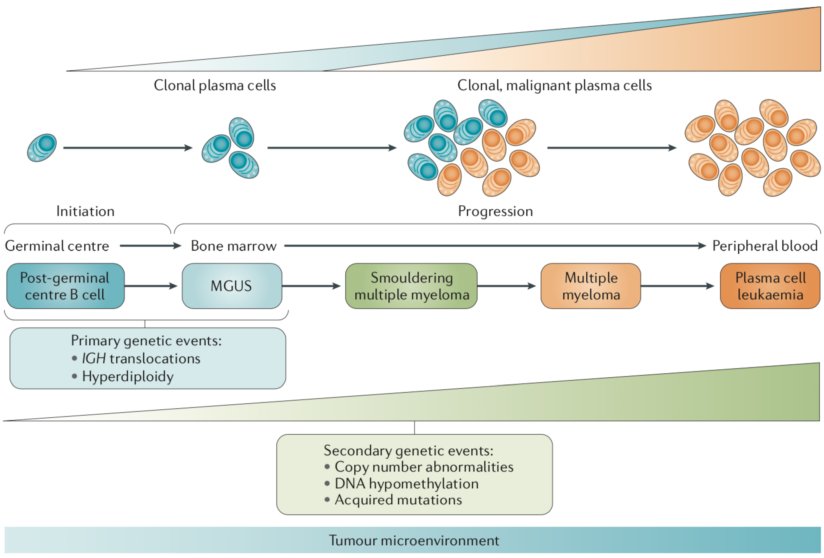

Kumar et al., 2017 NATURE REVIEWS | **DISEASE PRIMERS**

Fig. 1: **Development of monoclonal gammopathies**. The development of multiple myeloma is a multistep process, which starts with precursor disease states, such as monoclonal gammopathy of undetermined significance (MGUS) and smouldering multiple myeloma (SMM). Although MGUS, SMM and multiple myeloma are clinically well defined, many biological similarities between these disease states have been found. Multiple myeloma can progress to bone marrow-independent diseases, such as extramedullary myeloma and plasma cell leukaemia.

1.2 Microenvironment and TAMs: role in tumor progression

The interplay between multiple myeloma cells and the bone marrow microenvironment is crucial for myeloma development and progression of haematopoietic cells such as B cells, T cells, natural killers, myeloid-derived suppressor, osteoclasts (which have a role in bone resorption) and non haematopoietic cells, including bone marrow stromal cells and osteoblasts secreting several factors which contribute to proliferation of multiple myeloma cells, and can also contribute to bone damage. Endothelial cells might have a role in multiple myeloma cell migration. Bone disease in patients with multiple myeloma is caused by both increased activity and number of osteoclasts and reduced activity and number of osteoblasts. Indeed, the interaction of multiple myeloma cells with bone marrow stromal cells and osteoblasts causes increased production of RANKL and reduced levels of osteoprotegerin [16]. RANKL binds to RANK (receptor activator of NF-ϰB; also known as TNFRSF11A), which is expressed by preosteoclasts, resulting in increased differentiation to osteoclasts. Imbalance concering number and activity of osteoclasts and osteoblasts results in bone destruction and the development of bone disease [17].

Also, factors produced in the microenvironment can be associated with angiogenesis. Indeed, vascular endothelial growth factor A (VEGFA), which is produced by bone marrow stromal cells, is a strong angiogenic factor, resulting in increased oxygen supply through increased, local abundance of blood vessels [18].

The tumor microenvironment is a heterogeneous tissue that in addition to tumor cells, contain tumor-associated cell types such as immune cells, fibroblasts, and endothelial cells. Significant alterations in its composition and structure create a permissive environment for tumor growth, invasion, and dissemination. Among tumor-infiltrating immune cells, tumor-associated macrophages (TAMs) are educated to exert important biological functions that profoundly affect tumor initiation, growth, and dissemination. Tumour-associated macrophages (TAMs) are a major immune component of many types of cancer. TAMs promote tumours by secreting proangiogenic and growth factors, suppressing T-cell effector functions by releasing immunosuppressive cytokines and by affecting T-cell metabolism. Macrophages exerting these protumourigenic functions are termed M2- like macrophages, in contrast to the antitumourigenic M1-like subtype. The presence of TAMs correlates with poor prognosis in various types of human cancers [14]. Indeed, macrophages are an essential component of both innate and adaptive immunity and play a central role in host defence and inflammation. It is well known that activated macrophages are divided into two subsets, classically (M1) and alternatively (M2) activated macrophages. The M1 phenotype is characterized by the expression of pro-inflammatory cytokines, such as interleukin-12 (IL-12), IL-23 and tumour necrosis factor-a (TNF-a), as well as high reactive oxygen intermediate production. In contrast, cells of the M2 phenotype typically produce IL- 10 and IL-1 receptor antagonist (IL-1Ra) and have high levels of scavenger factors. M1 macrophages have been shown to have strong anti-bacterial and anti-tumour effects. In contrast, M2 macrophages are thought to have immunoregulatory functions promoting tissue remodelling and tumour progression [6].

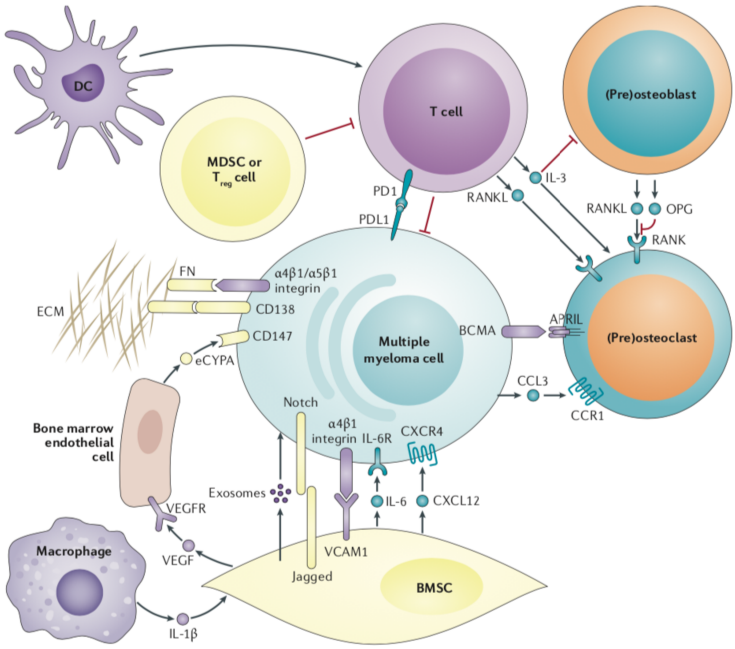

Kumar et al., 2017 NATURE REVIEWS | **DISEASE PRIMERS**

Fig. 2: Interplay between myeloma cells and tumor microenvironment. Central in the multiple myeloma microenvironment is the bone marrow stromal cell (BMSC), which is instrumental in creating a favourable niche for multiple myeloma growth. Indeed, the physical interaction of vascular cell adhesion protein 1 (VCAM1) on the cell surface of BMSCs and integrin on the myeloma cells results in the secretion of several cytokines, which favour myeloma cell proliferation and inhibit apoptosis. Macrophages in the microenvironment produce a wide range of factors, including IL-1β, which act on stromal cells and induce IL-6. Several cell types, including BMSCs, T cells, B cells, monocytes and multiple myeloma cells, produce IL-6, which promotes proliferation of multiple myeloma cells and resistance to apoptosis.

2. Bortezomib in Multiple Myeloma

Two important classes of drugs for the treatment of multiple myeloma are immunomodulatory drugs and proteasome inhibitors. The sensitivity of multiple myeloma cells to bortezomib and other proteasome inhibitors is related to the balance between the load and the capacity of the proteasome. Indeed, plasma cells are antibody- producing cells, so they have a physiological induction of the unfolded protein response to accommodate for antibody production. Multiple Myeloma is sensitive to therapies that increase stress on protein turnover, such as proteasome inhibition. Otherwise, overexpression of proteasome subunits and higher proteasome capacity were linked to resistance to bortezomib. In addition, differentiation plasticity in multiple myeloma cells might be related to bortezomib resistance [19]. Bortezomib (Velcade®) is a dipeptidyl boronic acid that selectively inhibits the ubiquitin proteasome pathway, which plays a role in the degradation of many intracellular proteins. It is the first-in-class selective and reversible inhibitor of the 26S proteasome: a multisubunit protein that degrades proteins involved in multiple cellular processes, including cell-cycle regulation, transcription factor activation, and apoptosis [20]. Bortezomib exerts anti-myeloma activity when it is used as a single drug or in combination with other anti-cancer agents in both patients with previously untreated MM and in patients with relapsed/refractory MM. It realizes its antiproliferative and antitumor activity by inhibiting the proteasomal degradation of several ubiquitinated proteins. This inhibition is achieved by bortezomib binding to the catalytic site of the 26S proteasome, which it achieves with high affinity and specificity. Bortezomib treatment has been associated with induction of mitochondrial depolarization and apoptosis [21]. Also, proteasome inhibition results in increased intracellular levels of p27 and p53; in addition, bortezomib also induces cell death through the inhibition of nuclear factor-κB activity, accumulation of misfolded proteins, the activation of c-Jun N-terminal kinase, and stabilization of cell-cycle inhibitors [19]. Although bortezomib treatment has generally offered encouraging results, primary and secondary resistance are emerging problems, with most patients demonstrating drug- resistant relapse following long-term treatment. In addition, primary resistance is also observed and refractoriness to bortezomib is a negative prognostic factor [21]. Resistance has been attributed to several factors, including genetic mutations, clonal evolution of MM cells, and bone marrow microenvironment changes. In preclinical studies, upregulation of the proteasomal system in bortezomib- resistant acute myeloid leukemia (AML) and MM model cell lines has been observed [22], [23]. Increased expression of the proteasome maturation protein has been observed in cell lines resistant to bortezomib.

Increasing proteasome maturation protein expression is essential for biogenesis of the proteasome, and its increased expression is one way by which bortezomib resistance is acquired. Another protein associated with resistance to bortezomib is the X-box binding protein 1 (XBP1), which is a transcription factor necessary for the final maturation of plasmablasts to plasmocytes and the secretion of immunoglobulin. X-box binding protein 1 also regulates the UPR mechanism by activating genes necessary for UPR activation. Low levels of XBPS1 gene expression have been found to correlate with a lack of sensitivity to bortezomib treatment. [19]; [24]. Cells displaying XBP1 gene mutations lose their sensitivity to bortezomib, thus resulting in the acquisition of disease resistance. Finally, PL5 gene expression is also a biomarker associated with response to bortezomib therapy: the RPL5 gene itself was identified in 20–40% of patients with MM and its low expression was found to correlate with longer PFS in patients with MM treated with bortezomib [19]. In addition, low RPL5 expression levels correlated with longer survival in newly diagnosed and relapsed patients treated with bortezomib.

3. Mechanisms of cancer resitance

3.1 Oxidative stress

As far as concerns the mechanisms of pharmacological resistance, several hypotheses and pathways have been advocated. Deregulated redox balance of cancer cells have been proposed as a possible mechanism of chemoresistance. To this regard, cancer cells exhibit persistent reactive oxygen species (ROS) levels that lead to adaptive stress responses and allow cancer cells to survive with elevated levels of ROS preserving cellular viability [25]. This activated intracellular ROS-scavenging system could have detrimental effects on anticancer drugs, since they work through accumulation of ROS to stimulate cytotoxicity and cell death. A part from ROS formation, MM cells are characterized by a very high overall level of protein synthesis due to production of a monoclonal immunoglobulin that [26] lead to endoplasmic reticulum (ER) stress and are dependent on the unfolded protein response (UPR) for maintenance of protein homeostasis [27], [28]. As long as oxidative stress occurs, cell triggers a complex series of biochemical cascades leading to the upregulation of antioxidant systems in the attempt to maintain the cellular redox balance. Among these various mechanisms, the heme oxygenase (HO) system is emerging as an important regulator of cancer cell redox balance [29], [30]. In the last decades, tumor metabolism has drawn increasing attention in the scientific world. Deregulated metabolism is a hallmark of cancer and recent evidence underlines that targeting tumor energetics may improve therapy response and patient outcome.

Despite the general attitude of cancer cells to exploit the glycolytic pathway even in the presence of oxygen (aerobic glycolysis or "Warburg effect"), tumor metabolism is extremely plastic, and such ability to switch from glycolysis to oxidative phosphorylation (OxPhos) allows cancer cells to survive under hostile microenvironments. Recently, OxPhos has been related with malignant progression, chemo-resistance and metastasis. Instead of using an oxidative metabolism like most of normal cells, cancer cells convert glucose into lactate even in presence of high oxygen tension [31]. Indeed, fermentation to lactic acid and the glycolytic breakdown of glucose generate a number of substrates which turn into "anabolic" precursors for the synthesis of different compounds, such as glucose-6-phosphate for glycogen and ribose 5-phosphate, dihydroxyacetone phosphate for triacylglyceride and phospholipids, and pyruvate for alanine and malate. Metabolite accumulation up- stream pyruvate production is further increased by the up-regulation of the low activity M2 isoform of pyruvate kinase (PKM2), that slows down the last step of glycolysis. In this respect, intermediate components of the glycolytic pathway appear to be more significant than its final product pyruvate. Given the limited pyruvate supply, to replenish the tricarboxylic acid cycle (TCA) cancer cells increase glutamine consumption, a key nutrient that provides carbon for acetyl-CoA, citrate production and lipogenesis, nitrogen for purine, pyrimidine and DNA synthesis, and reducing power in the form of NADPH to support cell proliferation [32]. The particular attitude of proliferating cancer cells to use aerobic glycolysis favors a microenvironment enriched in lactate and protons, with a subsequent pH reduction. Moreover, the large amount of lactate released by tumor cells can be taken up by normal stromal cells to regenerate pyruvate, which in turn can be extruded to refuel cancer cells [33]. The reduction in oxygen tension that characterizes proliferating tumor tissues, stimulates the hypoxia-inducible factor α (HIF1α), which drives the anaerobic glycolysis. This leads to lactate dehydrogenase A (LDH-A)-dependent lactic acid production, and the upregulation of monocarboxylated transporter (MCT)- 4 and of sodium-proton exporters to avoid intracellular acidosis. As a direct consequence, both aerobic and anaerobic glycolysis adopted by cancer cells contribute to the acidification of tumor microenvironment [34]. As an additional aspect, it has recently reported that acidic cancer cells undergo a metabolic change characterized by the acquisition of a more clear OxPhos phenotype through the inhibition of HIF1α expression, associated with a reduced proliferation compared to standard pH condition [35]. Tumor cells are extremely plastic even in terms of cellular energetics and may shift their metabolic phenotypes to adapt to microenvironmental changes, giving a selective advantage to cancer cells under unfavourable environments [36].

3.2 HDAC6: role in autophagy and immunomodulation

Concernig activation of cellular machanisms involved in cancer progression it has been focused attention on autophagy. Autophagy is a process for clearing malformed and damaged proteins within the intracellular compartment into autophagosomes for delivery to lysosomes for degradation and recycling. Also, autophagy can serve two key functions: a tumour-suppressive function through elimination of oncogenic proteins, and perhaps for established cancer, a tumour-promoting function via recycling of metabolites to maintain mitochondrial functionality [37]. It is the therapeutic role of autophagy-targeting drugs in cancer that is receiving recent attention due to the potential of such therapies to induce apoptosis or by-pass apoptosis defects to induce other forms of cytotoxicity. Enhanced autophagy can ensue following chemotherapy, and inhibition of autophagy under such conditions can lead to increased cell death as a cellular response to avoid accumulation of toxic proteins [38]. Autophagy is widely thought to contribute to proteasome inhibitor resistance in myeloma by providing an alternative pathway for clearance of dysfunctional proteins. Cells can also attenuate accumulation of dysfunctional proteins through decreased protein translation via the unfolded protein response (UPR) which is a conserved pathway that operates to prevent or correct a cellular phenotype termed endoplasmic reticulum (ER) stress via an adaptive response through a specific gene transcription programme. UPR and autophagy are thought to control cell viability in cells where abnormal protein homeostasis persists [39]. To date, only a limited number of inhibitors are available for the study of autophagy *in vitro* and *in vivo*. The anti- malarial agent chloroquine (CQ) that blocks lysosome acidification has been evaluated pre-clinically and in patients alone and in combination with chemotherapy for autophagy inhibition [40], [8]. Antagonists of the phosphoinositide 3-kinase- mammalian target of rapamycin pathway have also been tested as autophagy inhibitors. In particular, 3-methyladenine and 3-MA derivatives with improved solubility have been tested and show activity in vitro. Lastly, histone deacetylase 6 (HDAC6) inhibitors and pan-HDAC inhibitors have been evaluated as autophagy inhibitors. HDAC6 is involved in ubiquitin-dependent or ubiquitin-independent protein aggregate formation, as well as their clearance via autophagy [11]. HDAC6, in association with the dynein motor complex, recruits and transports misfolded polyubiquitinated proteins via the microtubule network to aggresomes/autophagosomes for subsequent degradation by lysosome [12]. Pan-HDAC inhibitors combined with bortezomib are potent in resistant cancers due to the complementary roles of the autophagy and proteasome pathways in protein recycling; however, such combination is poorly tolerated clinically [13].

HDACs have been recently addressed as epigenetic modifiers in regulating immune-modulatory pathway. However, their roles in regulating the immune-related pathways have not been observed completely [41]. Hence, the generation of selective HDACi and mechanistic insight into their role in the immune response against cancer cells is highly desirable goals and has the potential to augment anti-tumor immunity. Under such context, it is reported that the pharmacological and genetic inhibition of HDAC6 resulted in modulation of expression of co-stimulatory molecules, especially the tumor-associated antigens and MHC class I. Moreover, it seems that HDAC6 is a crucial regulator in the STAT3 pathways [42], which can be commonly activated in cancer, like osteosarcoma and other malignancies [43]. Authors reported that HDAC6 plays a role in regulating the co-inhibitory molecule PD-L1. This protein is one of the natural ligands for the PD-1 receptor present on T cells, which suppresses T-cell activation, proliferation, and induces T-cell anergy and apoptosis [43]. PD-L1 is found in cancer cells by many important studies [44], [45], and its overexpression is usually related to the poor prognosis of respective malignancies, including osteosarcoma [46], ovarian [47], gastric [48], and breast cancer [49].

3.3 Iron homeostasis deregulation

Iron is the most abundant element by mass on the Earth and is a growth-limiting factor for virtually all organisms. Considering the poor bioavailability of iron, the interplay of different proteins involved in iron import, storage, and export has to be tightly regulated, as there is no excretory route for excess iron. The ability of iron to get oxidized or reduced enables iron to take part in free radical generating reactions, as Fenton reaction in which ferrous iron donates an electron to hydrogen peroxide to produce the hydroxyl radical, a highly reactive oxygen species. As a result, iron is potentially mutagenic by causing DNA strand breaks, which provokes cellular transformations, or induces protein as well as lipid modifications within malignant cells. In turn, this may cause a more aggressive tumor cell behavior [15], [50], [51]. Mammalian cells require sufficient amounts of iron to satisfy metabolic needs and accomplish specialized functions. Only to mention a few, DNA polymerases and helicases contain iron-sulfur groups that rely on iron as essential co-factors [52]. In addition, cellular iron availability not only controls mitochondrial respiration, but also affects citric acid cycle enzymes [53], [54]. The malignant cancer phenotype is often found in association with a deregulated iron homeostasis, particularly the expression of iron-regulated genes that fuel their higher metabolic iron demands needed for division, growth, and survival [25].

This surplus of iron is needed not only during early steps of tumor development, enhanced survival [26] and proliferation of transformed cells [27], but also during late stages to promote the metastatic cascade. Iron is crucial in remodeling the extracellular matrix and increasing the motility and invasion of cancer cells [8]. A dysfunctional or deregulated iron metabolism in cancer patients often results in a decreased red blood cell (RBC) count and anemia is detected in approximately 40–70% of all cancer patients [4], [30]. Furthermore, cancer-induced anemia as well as inflammation-associated anemia is characterized by reduced erythropoiesis. Mechanistically, cancer-induced anemia is caused by the secretion of inflammatory factors, such as tumor necrosis factor (TNF)-α and interleukin-6 (IL-6). They inhibit erythropoiesis due to iron restriction in the reticuloendothelial system [32]. A growing number of studies explore the role of iron-related proteins in the context of cancer. Apparently, the expression of different iron-regulated genes such as the transferrin receptor (TfR1), ferritin light chain (FTL) [55], and the iron regulatory protein (IRP)-2 [40] in tumor cells correlated with a poor prognosis, a higher tumor grade, and increased chemoresistance. Given the complex network of iron regulatory genes in cancer cells and their role for tumor growth and survival, a better understanding of their regulation and interplay is needed. The identification of recently acknowledged iron-regulated genes, as lipocalin-2 (Lcn-2) as well as siderophore-binding proteins, might help to understand how the tumor exploits systemic and local iron management. Circulating iron is normally found complexed in transferrin (Tf), circulating in the bloodstream. Tf is taken up in peripheral tissue by binding to the TfR1. The ligand–receptor complex is endocytosed and recycled within the endosome, releasing ferric iron, which is exported into the cytosol by the divalent metal transporter (DMT)-1. High TfR1 expression correlated not only with a reduced response to chemotherapy [38], but also increased phosphorylation of src in breast cancer, promoting tumor cell division or adhesion. Moreover, the homologous TfR2 is also frequently upregulated in cancer cells [7]. Therefore, the Tf/TfR system not only enhances iron uptake, but also provokes tumor cell survival. Ultimately, tumor cells adjust intracellular iron metabolism to favor iron accumulation, by increasing iron uptake and storage, at the same time decreasing iron export. Imported iron enters the bioactive labile iron pool (LIP), which provides it for proliferative purposes. The amount of the LIP is sensed by post-transcriptional mechanisms of cytosolic iron-regulated RNA binding proteins 1 and 2 (IRP-1 and IRP-2) to fine-tune uptake, storage, and release of iron. When intracellular iron is low, IRPs interact with conserved iron-responsive elements (IREs) in the untranslated regions (UTRs) of central genes accounting for iron homeostasis.

Iron, when neither metabolically used nor stored in FT, is exported from cells to the circulation by the iron exporter ferroportin (FPN), gets oxidized by ceruloplasmin or hephaestin, and is loaded to Tf. The FPN efflux system represents one of the key mechanisms to adjust the iron amount in the body and to affect the ratio of stored and released iron [52, 53]. In invasive tumor areas, iron export via FPN is lower compared to normal tissue, with the notion that FPN expression in carcinomas inversely correlated with patient survival and disease outcome [54]. A decreased FPN expression in tumor cells is associated with enhanced availability of LIP-associated iron. Authors reported that this effect increased tumor growth in a breast cancer xenograft model, correlating with the aggressiveness of breast cancer subtypes. The expression of FPN is regulated by the acute-phase protein hepcidin, which induces internalization and degradation of FPN upon its binding, thereby attenuating the iron export capacity [4]. Finally, Peripheral tissues also secrete hepcidin, which, unlike liver-secreted hepcidin, is thought to act locally. Tissue sequestration and systemic iron levels are regulated by hepcidin, by controlling FPN-facilitated iron release into the plasma of all cells that handle iron, including intestinal enterocytes, hepatocytes, and macrophages [54].

3.3.1 Iron in tumor microenvironment

The role of iron for cancer development is tightly linked to its ability to modulate innate adaptive immune responses of macrophages or T cells. In order to control iron availability, immune cells adapt their phenotype accordingly to defend the host against invading pathogens. Since tumor cells might be recognized as foreign in the first place, it is not surprising that tumor cells compete for iron with immune cells of their local microenvironment. The inflammatory nature of the tumor microenvironment and the presence of inflammatory stimuli are critical regulators of iron availability. During early stages of carcinogenesis, pro-inflammatory cytokines endorse iron sequestration in macrophages and enhance the production of reactive oxygen species as a firstline anti-tumor defense. However, chronic inflammation or smoldering inflammation often creates an equilibrium between killing of immunogenic tumor cells and immune tolerance, inflammation often creates an equilibrium between killing of immunogenic tumor cells and immune finally driving tumor outgrowth. Outgrowth is supported as tumor cells often evade recognition or even acquire an immunosuppressive phenotype [56].

Based on the interplay between tumor cells and tumor-infiltrating immune cells, the latter ones are educated to a tumor-supportive, anti-inflammatory phenotype that significantly promotes tumor neovascularization, metastasis, growth and survival [56]. In contrast to the iron sequestration phenotype of inflammatory macrophages induced by pro-inflammatory cytokines, anti-inflammatory macrophages and lymphocytes show an iron release phenotype, donating and distributing iron within the tumor microenvironment [57]. In addition, macrophages are capable of ferritin secretion, whereby tumor growth is promoted. The appearance of tumor-supporting, iron-donating immune cells, in particular macrophages, is associated with tumor size and aggressiveness as well as poor patient prognosis [58]; [59]. Since macrophages are characterized by high functional plasticity and heterogeneity of activation, it is speculated that distinct macrophage subpopulations are found within the same tumor, with the individual phenotypes coined by their localization and microenvironmental stimuli [60]. Therefore, it seems appropriate to consider polarization of the TAM as a continuum of functional activation phenotypes [61] rather than distinct subpopulations. These observations also hold true for the iron-regulated gene signature of distinct macrophage phenotypes. The profile can be characterized by expression of a particular subset of iron-regulated genes to take up iron, store it, or export it in order to donate it to neighboring cells. Pro-inflammatory macrophages are prone to iron retention. They display an iron sequestering phenotype characterized by enhanced iron uptake and storage, but attenuated release [62]. In contrast, anti-inflammatory macrophages are predisposed to iron export and the distribution of iron to the extracellular space, whereas iron storage is reduced. As alternatively activated macrophages scavenge senescent and/or apoptotic cells [63], they play an important role in tissue repair, regeneration, resolution of inflammation, and iron recycling. Consequently, they show a high expression of scavenger receptors such as CD163 and CD91. This allows for the uptake of iron-containing heme clusters, which in turn enhances the expression of heme oxygenase 1 (HO-1). The iron-release phenotype is associated with upregulation of the iron exporter FPN, while the iron storage protein FT is downregulated. The majority of the heme-recycled iron joins the LIP, with only a small proportion actually being stored in FT. Non-heme-bound iron can be taken up through the DMT-1. These features allow anti-inflammatory macrophages to rapidly mobilize and redistribute iron to the local microenvironment in order to support the demand of surrounding cells. This iron-donating macrophage phenotype was directly linked to enhanced tumor cell proliferation and growth, both in vitro and in vivo. Recently, has been provided that TAM adopt an iron-release phenotype due to their interaction with dying tumor cells, whereby iron availability was increased within the tumor microenvironment.

Under these conditions, TAM expressed higher levels of the high-affinity iron-binding protein lipocalin-2 (Lcn-2). Lcn-2 turned out to export iron from TAM, while depletion of the established iron exporter FPN did not alter their iron release capacity. These observations suggest the existence of an alternative iron transport pathway in the tumor microenvironment, operating independently of FPN. Since tumors demand an excess of iron, both during early steps of tumor development and late metastatic processes, recent paradigms of macrophage iron polarization are of clinical interest. The fact that TAMs actively release iron to the tumor microenvironment positions them at the center of pathways associated with the concepts established as the "hallmarks of cancer". Iron handling in the tumor microenvironment emerged as an important aspect of tumorigenesis. Cancer cells reprogram their iron metabolism to increase net iron influx. This is accomplished by upregulating proteins for iron uptake such as Tf. The Tf/TfR system represents one of the major routes for iron acquisition, both in normal and malignant cells [64]. Upregulation of this highly conserved iron acquisition pathway is found in a variety of cancers, including breast and colon. Thus, it appears logic to apply an anti-TfR strategy as a therapeutic measure. Studies revealed that anti-TfR treatment was specifically encouraging for therapeutic approaches in hematologic cancer due to the fact that cells of the hematopoietic lineage are highly iron-dependent. At the same time, these observations raised major concerns for the use of anti-TfR antibodies for the treatment of other tumor types. The problem may arise that maturing erythroid cells would severely be affected by anti-TfR antibodies, which, in turn, may disturb erythropoiesis and cause anemia. variety of studies confirmed an improved anti-cancer drug uptake upon conjugation to a TfR monoclonal antibody. Not only to mention that TfR expression is significantly upregulated on cancer cells, it also represents a very effective receptor-mediated endocytosis system. Therefore, the Tf–TfR system is considered a promising target to enhance the uptake of drugs that are specifically conjugated to Tf to be recognized by the TfR and to facilitate uptake in, i.e. multidrug-resistant tumor cells [65]. It needs also consideration that cancer cells might have evolved alternative strategies to take up iron trough unappreciated transport proteins. Lcn-2 might accomplish such a role due to its ability to scavenge iron-loaded siderophores. Siderophores are small, low-molecular-mass iron-binding ligands known from iron acquisition mechanisms used by bacteria. Interestingly, higher organisms such as fungi or mammals are also able of producing this type of iron-scavenging molecules. Lcn-2 shows an extra ordinary high affinity to bind iron-loaded catecholate-type siderophores. However, it still remains unclear if siderophores are indeed produced in mammals to mediate Lcn-2–iron binding or if Lcn-2 takes advantage of bacterial siderophores, residing within mammals from e.g., commensal bacteria.

A recent study proposes that bacterial siderophores do not only serve as iron scavengers to limit bacterial growth but are also able to support the host's iron homeostasis. Lcn-2 is recognized and internalized by cells via their highly expressed high-affinity Lcn-2 receptor (Lcn-2R) and/or the low-affinity megalin receptor. Several studies in humans suggest Lcn-2 as a pro-tumorigenic factor in breast cancer, correlating with a decreased survival and reduced responsiveness to neoadjuvant chemotherapy [65]. It has been observed that human breast tumors contain enhanced amounts of Lcn-2, especially during advanced stages. Additionally, experimental transgenic tumor-bearing mouse mammary tumor virus (PyMT) mice exhibit higher Lcn-2 plasma levels compared to controls, and Lcn-2-deficient PyMT mice developed fewer tumors than Lcn-2-competent littermates [66]. These observations strengthen the concept that Lcn-2 promotes its pro-tumor functions via Lcn-2R signaling. Lcn-2 was also shown to induce epithelial-to-mesenchymal transition (EMT) through upregulation of the EMT-associated transcription factors Snail1, Slug, and Twist1, which, in turn, influence the expression of epithelial and mesenchymal markers to promote invasiveness. While the majority of studies so far focused on mechanisms promoted by tumor cell-derived Lcn-2, recent data from our group suggest that stromal Lcn-2 promoted metastasis by enhancing EMT and lymphangiogenesis. In fact, it was speculated that the iron load of Lcn-2 defines pro-tumor characteristics of Lcn-2. However, it is still unknown how tumor cells selectively take up iron-loaded Lcn-2 relative to iron-free Lcn-2 or how the latter is antagonized within tumor cells in order to avoid its reported apoptotic effects [66].

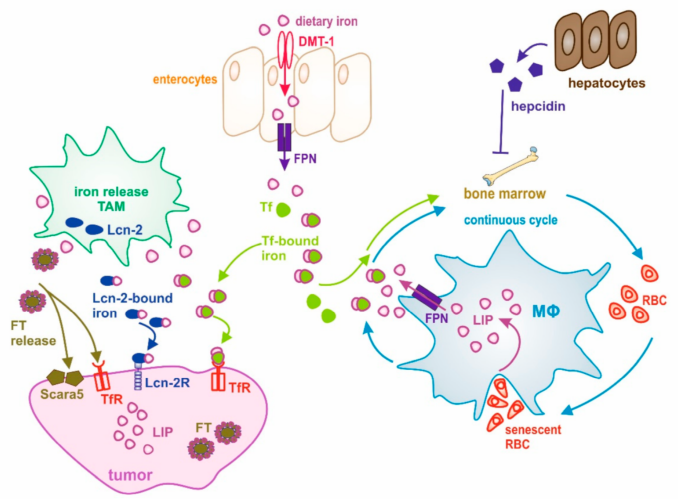

Michaela Jung; Int J Mol Sci. 2019

Fig. 3: schematic overview of iron homeostasis in tumor. Divalent metal transporter 1 (DMT-1); ferroportin (FPN1); transferrin (Tf); senescent red blood cells (RBCs; labile iron pool (LIP); tumor-associated macrophages (TAM); Tf receptor (TfR); lipocalin-2 (Lcn-2); high-affinity receptor Lcn-2 (Lcn-2R); ferritin (FT); Scara5 (FTL).

3.3.2 Iron in Multiple Myeloma

Iron metabolism is significantly altered in multiple myeloma (MM). Availability of iron for the developing erythrocytes becomes limiting resulting in the characteristic anemia so frequently seen in this disease. In contrast, the availability of iron for the expanding malignant clone remains a critical determinant of MM progression. Anemia is a frequent finding in myeloma patients. One large retrospective analysis of more than one thousand patients found that 73% of myeloma patients were anemic at the time of diagnosis with hemoglobin levels <12g/dl. The anemia typically worsens with disease progression and often improves during chemotherapy-induced response. The incidence and severity of anemia is less in the MGUS pre-malignant stage and in a more slowly progressive form of MM termed “smoldering” or “indolent” myeloma. Erythropoietic stimulating agents (ESAs) have been commonly used for the treatment of anemia of multiple myeloma (as well as other malignancy-associated anemias) [67]. Although numerous trials have examined the efficacy of erythropoietin derivatives in the treatment of myeloma-associated anemia, the overall impact and cost effectiveness of such treatment remains controversial. Few of these trials were powered to detect significant differences in survival.

Response to ESAs is usually defined as an increase in hemoglobin of 2g/dL and response rates are consistently in the range of 60–70% (ranging from 35–85%) [68]; [69]. These trials demonstrated that rise in hemoglobin is due to the ESA therapy rather than change in status of the underlying myeloma. However, therapy with ESAs has been associated with increased risk of hypertension, antibody-mediated red cell aplasia and thromboembolic events. Targeting to a lower hemoglobin level may avoid some of these side effects. There are several potential etiologies for myeloma-associated anemia that have been considered. Certainly, the extensive BM involvement with malignant cells can theoretically result in decreased capacity for functional erythropoiesis. In addition, as mentioned above, production of erythropoietin in the presence of myeloma-associated renal insufficiency is depressed and is an accepted indication for ESA treatment. Also, It has been reported that malignant plasma cells have increased expression of Fas ligand on their surface which may cause apoptosis of erythroid precursors within the marrow [57]. Although these putative pathogenic mechanisms may contribute to myeloma-associated anemia, the characteristic iron studies in patients strongly support the notion that most patients suffer from the anemia of inflammation that previously was termed “anemia of chronic disease”. It is now understood that most of these cases show impaired iron utilization due to increased pro-inflammatory cytokines that stimulate the production of the iron-regulatory hormone hepcidin. Animal models have demonstrated that hepcidin (an acute phase reactant elevated in pro- inflammatory states) is the primary negative regulator of iron transport and release from macrophages and enterocytes [70]. Hepcidin, a liver-produced protein, binds to the iron exporter ferroportin, and ferroportin is then internalized and degraded [71]. The loss of ferroportin proportionately decreases the activity of the normal cellular pathway for iron efflux. Hepcidin expression is induced by infection or inflammation through pro-inflammatory cytokine signaling. Cytokine activation of the JAK/STAT or SMAD signaling pathways in hepatocytes results in stimulation of the hepcidin promoter and induction of hepcidin expression as part of the type II acute phase reaction. Interleukin-6 (IL-6) has been identified as the primary physiologic cytokine regulating hepcidin expression. Since several studies document heightened systemic IL-6 levels in patients with multiple myeloma, it was tempting to hypothesize that an IL-6-induced upregulation of hepcidin expression in patients was the major cause of anemia. The MM growth factor IL-6 was a candidate cytokine proximally stimulating hepatic synthesis of acute phase proteins in MM, including hepcidin. However, MM cells themselves rapidly and robustly respond to IL-6 with a stimulated gene expression program. In addition to IL-6, serum levels of TNF-alpha and IL-1beta are elevated in myeloma patients [59] and they both have been implicated in hepcidin regulation [61].

Data collectively support the idea that the growth of the MM clone within the bone marrow stimulates paracrine expression of BMP-2 and IL-6. The resulting elevated serum levels of these cytokines activate the hepcidin promoter in hepatocytes. Most promoter activation is due to BMP-2 signaling through SMADs to the BREs but IL-6 can also signal the promoter at its STAT3 binding site via the gp130/JAK/ STAT pathway with a synergistic interaction at the level of the hepcidin promoter to further enhance hepcidin expression. On the other and, TfR1 is overexpressed on cells with a high rate of proliferation including many types of cancer cells including malignant hematopoietic cells. Within the cell, iron is a required co-factor for the ribonucleotide reductase, an enzyme necessary for the conversion of ribonucleotides into deoxyribonucleotides that is essential for DNA synthesis and is also often overexpressed in cancer cells. Without iron this enzyme is rendered inactive leading to cell cycle arrest. Due to the high rate of proliferation and increased metabolism, cancer cells have an increased need for iron, making them more susceptible to the disruption of iron metabolism. Thus, direct iron chelation or blockage of iron uptake through the TfR have both been explored as potential cancer therapies [58]. One way to disrupt iron metabolism in cancer cells is the direct chelation of iron to deplete intracellular iron levels. The iron chelator desferrioxamine (DFO) produced by the bacterium *Streptomyces pilosus* has been used for the treatment of iron overload disease and has also shown anti-cancer effects. However, the utility of DFO is limited due to its poor membrane permeability and short plasma half-life. Many DFO analogs have been prepared in order to overcome these problems like the synthetic iron chelator di-2- pyridylketone-4,4-dimethyl-3-thiosemicarbazone (Dp44mT) or gallium. Blocking iron metabolism can also be accomplished through the use of antibodies targeting the TfR1. This strategy exploits the over-expression of the receptor in cancer cells. Additional potential disruptor of MM cell iron metabolism is curcumin. Clinical trials are currently evaluating curcumin in MM patients after some promising pre-clinical studies. Curcumin is a polyphenolic extract isolated from the spice turmeric (*Curcuma longa*). This plant extract is lipophilic, readily permeates cell membranes, and has been shown to have many beneficial properties including anti-inflammatory, antioxidant, and chemotherapeutic activity due to its complex structure and its ability to influence multiple cell signaling pathways can also bind iron and has been shown to be an iron chelator. Blocking iron metabolism can also be accomplished through the use of antibodies targeting the TfR1[64]. This strategy exploits the overexpression of the receptor in cancer cells and its central role in cancer cell pathology. Antibodies specific for the TfR1 that are directly cytotoxic to the cell through the induction of iron starvation can interfere with iron uptake in two ways.

They can be neutralizing antibodies in that they inhibit the binding of Tf to the receptor and thus block iron uptake and/or they can be non-neutralizing antibodies that still allow Tf to bind the receptor but induce iron deprivation by disrupting the normal cycling pathway of TfR1. Antibodies have additional anti-tumor mechanisms through their effector functions including antibody-dependent cell-mediated cytotoxicity (ADCC), antibody- dependent cell-mediated phagocytosis (ADCP) and complement-mediated cytotoxicity (CDC). In fact, the mouse/human chimeric antibody D2C specific for the TfR was shown to induce ADCC activity against human cancer cells. Furthermore, antibodies targeting the TfR1 have the added benefit of being able to act as delivery vehicles to internalize anti- cancer agents by receptor-mediated endocytosis, which can also potentially trigger a cytotoxic effect even if the antibodies do not have a direct anti-cancer effect [4]. Various antibodies targeting the TfR have shown anti-cancer effects against myeloma cells. The murine IgA anti-human TfR antibody 42/6 is cytotoxic to RPMI 8226 human MM cells *in vitro* [72]. This antibody inhibits binding of Tf to its receptor and additionally induces down-regulation of the receptor on the cell surface. The 42/6 therapeutic has been studied in a prior phase I clinical trial. Two antibodies avidin fusion proteins targeting the TfR have also been studied for their anti-myeloma effects. One of these fusion proteins is ch128.1Av (formerly known as anti-hTfR IgG3-Av) and the second one is anti-rat TfR IgG3-Av. Both of these fusion proteins consist of mouse/human chimeric IgG3 genetically fused to chicken avidin at the C_H3 domains of each heavy chain. These molecules were designed to be universal vectors that can deliver a wide variety of biotinylated therapeutic agents into cancer cells by receptor-mediated endocytosis. Additionally, both fusion proteins have been shown to exhibit superior intrinsic cytotoxic activity compared to their parental antibody without avidin against a variety of malignant hematopoietic cell lines, including myeloma cells of their respective species. Ch128.1Av was also cytotoxic to primary cells isolated from MM patients including a case of plasma cell leukemia (PCL), the most aggressive presentation of MM. Ch128.1Av significantly alters the classical recycling pathway of the TfR, redirecting it to lysosomal compartments, the site in which it is presumably degraded. As a result, the surface level of the TfR is dramatically reduced leading to lethal iron deprivation characterized by mitochondrial depolarization and activation of caspases 2, 9, 8, and 3 [72].

4. HDACs inhibitors: Classification and mechanisms of action

Epigenetic processes are a means of affecting gene expression without altering the nucleic acid (DNA) sequence. Deregulated HDAC activity is an epigenetic hallmark of cancer, resulting in aberrant gene expression and cellular signaling that promotes cell growth and survival, and resistance to apoptosis [73, 74]. Acetylation and deacetylation of histones catalyzed by histone acetyl transferases (HAT) and HDAC are one of the fundamental modification processes of biologic significance. Hyper-acetylated chromatin is transcriptionally active, and hypo-acetylated or deacetylated chromatin is transcriptionally silent. Transcriptional machinery is unable to access DNA when chromatin is condensed secondary to the removal of acetyl groups on core histones. Altering the acetylation of chromatin may thus alter the expression of oncogenes and tumor suppressors and that influences oncogenesis. In addition, specific DNA residues may be deacetylated, altering the binding of transcription factors. This may enhance or repress transcription altogether [75]. Besides the effect on the acetylation status of histones, HDAC inhibition also affects other cellular processes and can lead to a variety of biologic effects downstream important for cellular proliferation, angiogenesis, differentiation and survival. A total of 18 HDACs have been identified and grouped into four classes based on their homology to yeast HDACs, subcellular localization, and enzymatic activities [76]. The classes differ in tissue expression and protein targets [77]. Class I HDACs include HDAC1-HDAC3 and HDAC8, which are localized to the nucleus and primarily act on histone proteins and transcription factors. Class II HDACs include HDAC4-HDAC7, HDAC9, and HDAC10 [76]. They are thought to move between the nucleus and cytoplasm, where they act primarily on non-histone proteins. HDAC inhibition has been described as a master switch that could simultaneously affect multiple pathways critical for the survival of MM cells. As a class, HDACi inhibit the actions of HDAC enzymes and affect the expression of genes that regulate of cancer cell survival via a number of mechanisms. HDACi bind to the catalytic domains of HDACs, downregulating their activity, which in turn inhibits MM cell survival and proliferation[78]. Most HDACi arrest the cell cycle at G1-M phase [79] and induce apoptosis by upregulation of many proapoptotic proteins and downregulation of antiapoptotic proteins such as Bcl-2 [78]. HDACi have a number of direct and indirect effects that contribute to oxidative damage to cellular DNA. They cause delays in mitosis by overcoming the spindle assembly checkpoint through changes in tubulin. HDACi also inhibit hsp90, a cellular chaperone required for proteins involved in intracellular signaling (Raf, Her2/neu, ERK, NF-κB). HDACi also exhibit antiangiogenic effects and induce autophagy [80] cause acetylation of tubulin and disruption of aggresome formation and affect tumor immunity via effects on T cell receptor function, cytokine milieu of immune effector cells, and direct upregulation of proteins on malignant cells that enhance

cellular recognition by antigen presenting cells and other immune effectors. Proteasome inhibition in combination with aggresome inhibition by HDACi leads to cellular accumulation of proteins and hyperacetylation of tubulin, leading to apoptosis [81]. Transcription factor NF-κB translocates into the nucleus and promotes cell survival with transcription of various genes such as pro-inflammatory cytokines and anti-apoptotic proteins such as Bcl-2. Inactivation of NF-κB by deacetylase inhibition and proteasome inhibition result in synergistic apoptotic activity. Finally, HDAC inhibition allows for the expression of numerous tumor suppressor genes. Combination therapy with PI allows for a decreased breakdown of tumor suppressor proteins. Class I HDACi acetylate histone lysine residues, opening chromatin for protein synthesis and gene expression. HDACi that non-selectively inhibit a broad range of HDAC (pan-HDACi) [82] have been studied in MM and include panobinostat (PANO) and vorinostat (SAHA) [5, 83]]. HDACi that selectively target HDAC6 (HDAC6i), such as ricolinostat (ACY-1215) and ACY-241, increase acetylation of tubulin and disrupt transportation of aggresomes, and are being investigated for MM treatment [148,168]. Both preclinical and clinical data has supported the use of HDACI in combination with other agents, most strikingly with PI. Besides targeting the UPS and NF-κB, BTZ may target HDAC and may function as HDACi as well, further strengthening the rationale to use it in combination with HDACi [84] reported that BTZ can downregulate the expression of class I HDAC (HDAC1, HDAC2, and HDAC3) in MM cell lines at the transcriptional level accompanied by histone hyperacetylation. Short interfering RNA-mediated knockdown of HDAC1 enhanced BTZ-induced apoptosis, whereas overexpression of HDAC1 conferred resistance to BTZ in MM cells and administration of HDACi romidepsin restored sensitivity of HDAC-overexpressing cells to BTZ. Chen et al, [85] showed that, in vitro, the combination of HDACi with BTZ resulted in enhanced cellular killing compared with their effects as single agents. This synergy was associated with a reduction of NF-κB DNA binding activity, modulation of JNK activation, and a ROS-dependent downregulation of cyclin D1, Mcl-1, and XIAP. Inhibition of aggresomal pathway by HDAC6 inhibition, together with proteasomal inhibition by BTZ, also resulted in an accumulation of ubiquitinated proteins followed by synergistic anti-MM activity [83].

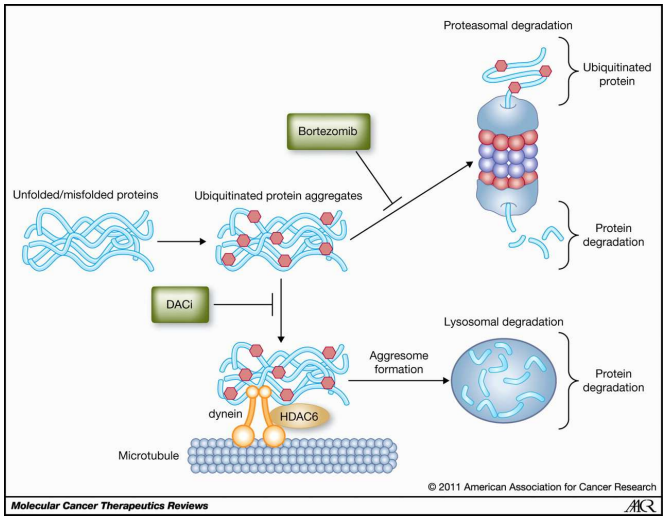

Fig. 4: Synergistic mechanism of action of Bortezomib and HDAC6i.

5. Zebrafish xenograft model of cancer and metastasis

In the last 30 years, the zebrafish has become a widely used model organism for research on vertebrate development and disease [72]. Through a powerful combination of genetics and experimental embryology, significant inroads have been made into the regulation of embryonic axis formation, organogenesis, and the development of neural networks. Research with this model has also expanded into other areas, including the genetic regulation of aging, regeneration, and animal behavior. Zebrafish are a popular model because of the ease with which they can be maintained, their small size and low cost, the ability to obtain hundreds of embryos on a daily basis, and the accessibility, translucency, and rapidity of early developmental stages. In the wild, D. rerio (Hamilton, 1822) are a tropical freshwater fish living in small rivers, streams, paddy fields, and channels in South Asia, including India, Myanmar, Bangladesh, and Nepal. Zebrafish prefer low-flow waters with vegetative overhangs that tend to have few predators [86]; [87]. The natural environments for zebrafish breeding are ponds that form during monsoons. Typically, these ponds are still and shallow with pebble, sand, or silt substrata that likely protects the clear eggs from predation. The breeding season correlates best to the onset of the monsoon season, although mature ova have been observed during the dry season. Thus, breeding is more likely to correspond to the more abundant availability of food during the monsoon season [87]. Zebrafish are hardy fish that lend themselves well to a laboratory environment. Successful husbandry relies on many of the properties of the natural habitat. Zebrafish live in clear, alkaline (pH 8.0) water with temperatures ranging from 20 to 33. Their diet in the wild consists mainly of insects, insect larvae, nematodes, and crustaceans [87].

In the laboratory, artificial food is typically supplemented with live food such as brine shrimp or mealworms for a more balanced diet. Many wild-type (WT), mutant, and transgenic strains of zebrafish are available through the Zebrafish International Resource Center in Eugene, Oregon (http://zebrafish.org/ home/guide.php) [21]. Excellent resources are available to guide a new zebrafish researcher, including The Zebrafish Book (Westerfield 2000), Zebrafish: A Practical Approach (Nusslein-Volhard and Dahm 2002), the Zebrafish Model Organism Database (http:// zfin.org), and a comprehensive review on zebrafish husbandry by Lawrence (2011). Zebrafish are prolific breeders, producing transparent embryos that allow researchers to study early developmental events in detail. Because the chorion and embryo are clear, zebrafish are particularly amenable to live-cell imaging to characterize cell morphology and cell division and migration patterns. Embryos develop rapidly, starting with synchronous divisions that subdivide the single blastomere, which sits on a yolk ball, into several thousand cells. By 24 hr, the embryos have a defined body axis and rudimentary organs, including a contractile heart. Zebrafish have a rapid generation time, reaching adulthood in approximately 3 months with an average lifespan of 2–3 years. Zebrafish are poised to provide advances in our understanding of the genetics and physiology of human disease. Because cellular changes can be followed in live animals, zebrafish are particularly useful for identifying the etiology and pathology of diseases that affect multiple tissues and organ systems, such as cancer, diabetes, atherosclerosis, and obesity. Orthologs for 82% of known human disease genes have been identified. The combination of mutant strains and inducible, reversible transgenes enables genetic approaches that closely mimic levels of gene expression characteristic of human disease. Zebrafish is already having an impact on diseases such as melanoma and other cancers, tuberculosis, autism, and cardiovascular disease [87]. Zebrafish model has been used to evaluate several factors involved in Multiple Myeloma progression, as bone marrow angiogenesis is associated with multiple myeloma (MM) progression. c-Myc has been postulated to be the master regulator of angiogenic factors, most prominently VEGF, and to be preeminent for the angiogenic switch required for tumor progression and metastasis [88]. Functional mechanisms of c-Myc mediating disease progression are not fully elucidated, and a role of c-Myc in triggering MM BM angiogenesis may be a contributing factor [89]. Jing Zhang et al. demonstrated the antiangiogenic activity of adaphostin, targeting c-Myc/Hypoxia-Inducible Factor-1α–Dependent Pathway. The zebrafish model shows equal capacities to discriminate antiangiogenic compounds more rapidly at 24 to 48 h with higher screening capacity.

Authors demonstrated the ability of adaphostin to mediate selective inhibition of angiogenic vassel sprounting in zebrafish embryos when used in low doses, establishing a xenograft zebrafish model for angiogenesis in MM [89]. Newer zebrafish multiple myeloma (MM) models have been developed to predict preclinical therapeutic efficacy of some compounds. Jianhong Lin et al. described a novel zebrafish model that supports the growth of both MM cell lines and primary MM cells and could provide an efficient, rapid, and inexpensive platform for drug screening and studying the biology of MM. Also, using transparent Casper zebrafish early-stage embryos (48 hpf), they suggested that the zebrafish embryo perivitelline space recapitulates the growth support provided by the human bone marrow microenvironment since it allows both myeloma cell lines and primary myeloma cells growth. They demonstrated whether this model could be used to assess efficacy of a known anti-MM agent. They also observed that cells from those patients with resistance to bortezomib and/or lenalidomide were also resistant to the same agents in our zebrafish model, validating the reliability of their system and confirming that primary MM xenografts can be used to predict patient responses to chemotherapy in vivo. The advantages of the system are the ability to use patient cells, the small number of MM cells required, the reduced variability between animals, the ability to perform medium-throughput in vivo drug screening using primary MM patient cells, and a short latency that may permit quick screening in real time [89] . Cell metastasis is a multistep process that involves several steps, including cell invasion, egress, passage into the circulation, and specific homing to predetermined distant tissues. The bone marrow (BM) is one of the most critical organs for cell dissemination and cell metastasis in solid tumors such as prostate, breast and lung cancers, and in hematologic cancers, including multiple myeloma (MM) and leukemia. A similar process occurs with cell trafficking of hematopoietic stem cells (HSC) in and out of the BM. MM represents a good model to examine homing to the BM as it presents with multiple lesions in the BM by the time patients present with their disease [89]. Intracardiac injection of tumor cells into zebrafish embryos is a useful new technique for rapid screening of cancer cells that can home or metastasize to the BM. There are recent evidences that many cytokines and chemokines are similar between zebrafish and that of mammals such as CXCL12, and that the hematopoietic role of the CXCR4–CXCL12 axis in zebrafish mirrors the functional role of CXCR4–CXCL12 in mammals [90]. Developing a zebrafish model for assessment of tumor cell homing and metastasis to the BM by injecting either MM cell lines or patient-derived MM cells into zebrafish embryos and demonstrating their homing to the caudal hematopoietic tissue (CHT) where the HSCs migrate after their emergence from the ventral wall of the dorsal aorta gained great interest in the last years.

Sacco et al. first demonstrated the homing ability of MM cells in CHT of zebrafish embryos, then they established the role of CXC4-CXCL12 axis in supporting the migration and adhesion of myeloma cells in the BM niche using zebrafish model. Injection in zebrafish embryos of CXCR4 silenced MM cells compared to control cells infected with a scrambled shRNA showed a significant reduction of the number of CXCR4 silenced MM cells homing to the CHT compared to control ones. Authors also showed the applicability and functional relevance of the zebrafish model in the context of another B-cell malignancy with specific tropism to the BM using a cultured cell line derived from a patient with Waldenstrom's macroglobulinemia. Injection of either CXCR4-overexpressing or CXCR4-silenced WM cells showed that increased CXCR4 expression in WM cells led to enhanced CHT-homing of WM cells whereas the homing of CXCR4-silenced WM cells to the CHT was reduced when compared with scrambled control [91]. Thus, zebrafish represents an efficient tool to study hematological malignances.

Aim

Chapter 1: HDAC6 enzymatic activity inhibition in Multiple Myeloma

It is well known that dysregulated HDAC activity is an epigenetic hallmark of cancer, resulting in aberrant gene expression and cellular signaling that promotes cell growth and survival, and resistance to apoptosis [74]. HDAC inhibition has been described as a master switch that could simultaneously affect multiple pathways critical for the survival of MM cells. As a class, HDACi inhibit the actions of HDAC enzymes and affect the expression of genes that regulate cancer cell survival via a number of mechanisms. HDACi bind to the catalytic domains of HDACs, downregulating their activity, which in turn inhibits MM cell survival and proliferation [78]. Also, HDACs have been recently addressed as epigenetic modifiers in regulating immune-modulatory pathway. However, their roles in regulating the immune-related pathways have not been observed completely [44]. In particular, it seems that HDA6 is involved in ubiquitin-dependent or ubiquitin-independent protein aggregate formation, as well as their clearance via autophagy and acts as a crucial regulator in the STAT3 pathways which can be commonly activated in cancer, like osteosarcoma and other malignancies. Authors reported that HDAC6 plays a role in regulating the co-inhibitory molecule PD-L1. This protein is one of the natural ligands for the PD-1 receptor present on T cells, which suppresses T-cell activation, proliferation, and induces T-cell anergy and apoptosis [92]. To this end, the first chapter of the research project focused on defining the role of HDAC6 enzymatic activity in MM cells and its link with activation of myeloma cells resistance mechanism to bortezomib treatment.

Chapter 2: Iron as key player on inducing myeloma cell resistance to bortezomib

Recently, the role of iron in tumor progression gained interest, since it is tightly linked to cancer cell metabolism and, also, modulates innate adaptive immune responses of macrophages or T cells. Among the mechanisms of cancer cell resistance, Fenton reaction, induced by free iron in cells, produce the hydroxyl radical, a highly reactive oxygen species. As a result, iron is potentially mutagenic by causing DNA strand breaks, which provokes cellular transformations, or induces protein as well as lipid modifications within malignant cells. In turn, this may cause a more aggressive tumor cell behavior. Concerning the role of iron in tumor microenvironment, it has been demonstrated that pro-inflammatory macrophages are prone to iron retention. They display an iron sequestering phenotype characterized by enhanced iron uptake and storage, but attenuated release.

In contrast, iron-donating macrophages in tumor microenvironment are associated with tumor size and aggressiveness as well as poor patient prognosis [58];[59]. Recently, it has been provided that TAM adopt an iron-release phenotype due to their interaction with dying tumor cells, whereby iron availability was increased within the tumor microenvironment. Under these conditions, TAM expressed higher levels of the high-affinity iron-binding protein lipocalin-2 (Lcn-2). Lcn-2 turned out to export iron from TAM, while depletion of the established iron exporter FPN did not alter their iron release capacity [64]. These observations suggest the existence of an alternative iron transport pathways in the tumor microenvironment. The second chapter of this research project focused on evaluation by which iron metabolism induces myeloma cells resistance to bortezomib and on understanding the interplay between iron metabolism in macrophages and myeloma cells in tumor microenvironment.

Material and methods

Cell culture and treatments

Myeloma cell lines (U266, OPM2, MM.1S) were cultured in RPMI 1640 medium supplemented with 10% FBS and 1% penicillin/streptomycin at 37 °C and 5% CO2. BTZ resistant cell line (U266R) was obtained alternating exposures first to 10 nM of bortezomib (BTZ) and drug-free culture medium for several weeks. To examine the response to BTZ in U266/BTZ-R, we performed experiments after that resistant cell line was regrown in drug-free medium for 3 days. Based on the previous literature data, 15 nM BTZ (Takeda, Rome, Italy) was used in all experiments [159]. To evaluate the the effects Tubacin (Sigma-Aldrich) on both U266 and U266R cells, alone or in combination with BTZ, cells were seeded in 6-well culture plate at density 5×10^5 cells per well (about 60% confluency). Treatments with Tubacin was performed up to 24h alone or in combination with BTZ. For viability assay, U266 cells were seeded on 96-well black culture plate (Eppendorf, Milan, Italy) at density 1×10^4 cells per well, and subsequently treated with 5μM 10 μM and 20uM with tubacin both of them alone and in combination with 15nM of BTZ. For estimation of iron induced effects, myeloma cells were pretreated with 200 μM Ferric Citrate Ammonium (FAC; Sigma- Aldrich) for 24h alone or in combination with BTZ 15nM. The iron chelator Deferasirox 50 μM (Exjade, NOVARTIS) was used to confirm the effects of iron in myeloma cells.

Sample collection

After written informed consent, samples were collected from healthy donors (HD) at Division of Hematology, AOU Policlinico – OVE, University of Catania. PB (Peripherical Blood) mononuclear cells were obtained after density gradient centrifugation on Ficoll and cultured in low-glucose Dulbecco's modified Eagle's medium supplemented with 10% heat- inactivated FBS, 100 U/ml penicillin, 100 mg/ml streptomycin and 1% L-glutamine. After 24 h in culture, non-adherent cells were removed, whereas mononuclear cells were treated with PMA 100nM to promote macrophage differenciation and selected by their adherence and morphology to the plastic-ware. The cultures were maintained at 7°C and 5% CO_2 .

Cell viability and apoptosis

Cell viability was assessed using XTT assay (Sigma, Aldrich) according to the manufacturers' protocol. Cells were seeded in a 96-well plate at a density of $1x10^5$ in 100ul and cultured for 24 and 48h. PMS 10mM was added to a solution of 4mg XTT immediately before labeling cells. 25ul of PMS/XTT solution was added to each well containing 100 ul of cell culture. Cell were incubated for 4h and cell viability was evaluated reading adsorbance at 450 nm, using MULTISKAN FC (Thermofisher scientific). Viability of the cells was expressed as percentage of vitality of untreated cell.

Evaluation of apoptosis was performed by flow cytometry. Samples ($5x10^5$ cells) were washed and resuspended in 100 μL of PBS. 1μL of A5-FITC solution and 5μl of dissolved PI (Beckmam Coulter, made in France) were added to cell suspension and mixed gently. Cells were incubated for 15 minutes in the dark. Finally, 400 μl of 1X binding buffer was added and cell preparation was analyzed by flow cytometry (MACSQuant Analyzer 10, Miltenyi Biotec).

Intracellular LIP estimation

Cells ($0.5x10^6$) were collected and washed with phosphate-buffered saline (PBS). Washed cells were incubated with CA-AM 0,5 μM (Sigma- Aldrich) for 15 minutes at 37°C. Cells were washed three times in PBS at 1500 rpm for 5 minutes and 100 μl of cell preparation was analyzed by flow cytometry (MACSQuant Analyzer 10, Miltenyi Biotec).

Citofluorymetric analysis of autophagy

Autophagic cells and formation of acidic vesicular organelles (AVOs) were quantified by FACS following acridine orange staining. Cells were washed with phosphate-buffered saline (PBS), 20 μg/mL solution of acridine orange in appropriate buffer were added to100 μL of cells suspension and incubated at room temperature for 20 min. Finally, the appropriate isotopic control was also included and labeled cells were acquired using a Beckman Coulter FC-500 flow cytometer.

Mitochondrial membrane potential DiOC2(3)

Cells were seeded at 1×10^5 cells/mL per plate in a 6-well plate and incubated for 24 h. Cellular mitochondrial membrane potential was assayed using the Muse MitoPotential Kit according to the user's guide. A total of 1×10^5 cells were collected by centrifugation (3000 rpm, 5 min) and washed with PBS. Supernatant was then removed and the cell pellets were stained with the Muse MitoPotential Kit (Merck Millipore, Guyancourt, France) for 25 min at 37 °C. The data was analyzed using the Muse™ Cell Analyzer Assay.

ROS analysis

To determine the intracellular ROS generation (mainly superoxide), cells were stained with 5 uM 5 μM of 2′,7′-Dichlorodihydrofluorescein diacetate (DCFH-DA, Sigma-Aldrich, prepared in ethanol and kept at −20 ◦C) at 37 ◦C and 5% CO2 for 30 min in the dark according to the instructions of the manufacturer. Samples were analyzed by cytometry using a 488 nm laser for excitation and detection at 535 nm. (FACS, FC500, Beckman Coulter, Milan, Italy)

Real-time RT-PCR for gene expression analysis

For each experiment, total RNA was extracted from cells using Trizol reagent and quantified using a UV spectrophotometer (NANODROP 1000, Thermofisher). One microgram of total RNA (in 20μL reaction volume) was reverse-transcribed in cDNA using reverse-transcriptase (Applied Biosystem) and oligo-dT primers in a standard reaction. The quantitative real-time polymerase chain reaction (RT-PCR) of the resultant cDNA was performed using a Applied Biosystem Sybr Green master,with 100 nM primers designed specifically for the transcripts of :hHMOX1; hDMT1; hFPN1; TFRC1 ; hPDL1; hND4; hCYTB ; hGLUT-S-TRANSF ; hTFAM; hLCN2; hIL-10; hHDAC6; hPCG1a (showed in table below) according to the gene manufacturer's recommended protocol (Applied Biosystem). Gene expression analysis of pro-inflammary and anti-inflammatory cytokines IL-10, TGFb, TNFa, CCL2 and ARG1 was performed using Go Taq Master (Promega) according to manufacturer's recommended protocol. Each reaction was run in triplicate. Samples were quantified accordingly (LightCycler analysis software, version 3.5) using the housekeeping gene GAPDH as standard.

hHMOX1 FW: AAGACTGCGTTCCTGCTCAAC	hHMOX1 RW: AAAGCCCTACAGCAACTGTCG
hDMT1 FW: TGCATTCTGCCTTAGTCAAGTC	hDMT1 RW: ACAAAGAGTGCAATGCAGGA
hFPN1 FW: CATGTACCATGGATGGGTTCT	hFPN1 RW: CAATATTTGCAATAGTGATGATCAGG
hTRFC1 FW: CCTGCACGTCGTCGCTTATA	hTFRC1 RW: ACCGAGTTTTGAGCGCTGTC
hLCN2 FW: TCACCTCCGTCCTGTTTAGG	hLCN2 RW:CGAAGTCAGCTCCTTGGTTC
hPDL1 FW: TTGCTGAACGCCCCATAC	hPDL1 RW:TCCAGATGACTTCGGCCTTG
hND4 FW: ACAAGCTCCATCTGCCTACGACAA	hND4 RW: TTATGAGAATGACTGCGCCGGTGA
hPCG1a FW: ATGAAGGGTACTTTTCTGCCCC	hPGC1a RW: GGTCTTCACCAACCAGAGCA
hTFAM FW: GGTCTGGAGCAGAGCTGTGC	TFAM RW: TGGACAACTTGCCAAGACAGAT
hCYTB FW: TCCTCCCGTGAGCGCGGTGA	hCYTB RW: AAAGAATCGTGTGAGGGTGGGACT
hGLUT-S-TRANSF FW: CTGGGCTTCGAGATCCTGTG	hGLUT-S-TRANSF RW:GGCAGACAAACTTCCACTGTC
hHDAC6 FW: GGAAAAGGTCGCCAGAAACTT	hHDAC6 RW: GGCCGGTTGAGGTCATAGTT
hSOD2 FW: GCATCAGCGGTAGCACCA	hSOD2 RW: GCAACTCCCCTTTGGCT
hGAPDH FW: TCCTGTTCGACAGTCAGCCGCA	hGAPDH RW: GCGCCCAATACGACCAAATCCGT

Flow cytometry evaluation of PDL1 and pSTAT3 in myeloma cells and immunomodulating cytokines in U937 cells and HD monocytes

To evaluate PDL1 espression and STAT3 phosphorilation in myeloma cells, cells were washed and respunded in 100 µl of PBS. 10 µl of PDL-1(cat. No 558065, BD Pharmigen) were added to each tube. Cells were incubated for 15 minutes at room temperature, protected from light. To measure pSTAT3 (cat. No 130-104-947) cells were permeabilized and fixed with PerFix nc- no centrifuge assay Kit (Beckman Coulter) according to manufacturer's recommended protocol. After centrifugation, cells were washed in 1ml of PBS and analyzed using flow cytometer (Beckman Coulter). To measure CD206, CD163, CD86, HLA-DR expression in U937 cells and in HD monocytes, cells were washed and respunded in 100 µl of PBS. 10 µl of anti-HLA-DR-PC5 (ref. No A07793, Beckman Coulter), CD206(MMR)-PE (ref. No IM2741), CD163-FITC (ref. No 333618, Biolegend) and CD86-PC7 (ref. No B30648, Backman Coulter) were added to each tube. Cells were incubated for 15 minutes at room temperature, protected from light. After centrifugation, cells were washed in 1ml of PBS and analyzed using flow cytometer (Beckman Coulter).

MitoTracker Mitochondrion-Selective Probe

To evaluate mithocondrial mass, cells were resuspended gently in prewarmed (37°C) staining solution, containing the MitoTracker (Invitrogen) probe at final concentration of 200nM. Cells were incubated for 30 minutes at 37°C and then washed three times with 1 ml of PBS buffer. 100uL of sample were analyzed by flow cytometry (MACSQuant Analyzer 10, Milteyi Biotec).

Immunofluorescence in myeloma cells

H929 LC3:GFP/mCherry cells were treated with FAC and bafylomicin and seeded in polysinitate coverslips before immunofluorescence. After washing with phosphate-buffered saline (PBS), cells were fixed in 4% paraformaldehyde for 20 minutes at room temperature. After fixation, cells were washed three times in PBS for 5 minutes. The slides were mounted with medium containing DAPI (4′,6-diamidino-2-phenylindole) to visualize nuclei. The fluorescent images were obtained using a Zeiss Axio Imager Z1 Microscope with Apotome 2 system and was performed by Image J Software.

Zebrafish husbandry

Zebrafish (*Danio rerio* H.) were obtained from the Zebrafish International Resource Center and mated, staged, raised and processed as described (Westerfield, 2000). The lines used *mfap4:Tomato* (Casper) (Walton E.M., 2015) *mpeg1:*cherryF;*tnfa*:eGFP (Wild type) (Mai Nguyen-Chi, 2015) have been previously described. The experiments performed comply with the Guidelines of the European Union Council (Directive 2010/63/EU) and the Spanish RD 53/2013. Experiments and procedures were performed as approved by the Bioethical Committees of the University of Murcia (approval numbers #75/2014, #216/2014 and 395/2017).

Cancer cell invasion/ metastasis test in zebrafish

To evaluate *in vivo* the role of iron in inducing myeloma cell resistance and its link with macrophages microenvironment, cancer cell invasion test was performed using *mfap4:tomato* casper larvae at 2dpf. U266 cells alone or treated with FAC 400uM for 24h were stained with Vybrant DiO cell labeling solution (Thermofisher) and injected in the Cuvier duct. To evaluate the role of macrophages to release iron and intact with myeloma cells, *mfap4:tomato* larvae 1dpf were dechorionated, treated with FAC 100uM for 24h and injected with U266 untreated (stained with

Vybriant DiO cell labeling). Microinjection was performed in all the experimental condition in larvae at 2dpf as follow:

- Wash $1x10^6$ cells with PBS+FBS 5%;
- Centrifuge at 1200 rpm for 5 minutes at 4°C;
- Resupend pellet in 1 ml of PBS+FBS 5% adding 5ul of Vybriant DiO labeling solution1mM;
- Incubate cells at 37°C for 15 minutes;
- Incubate cells on ice for 15 minutes;
- Centrifugate at 1200 rpm for 5 minutes at 4°C;
- Resuspend cells with 1ml of FBS 100%;
- Centrifugate cells at 1200 rpm for 10 minutes at 4°C;
- Wash twice with PBS+FBS 5% at 1200 rpm for 2 minutes at 4°C;
- Resuspend cells with 18ul PBS+FBS 5% adding 2ul of red phenol;
- Microinject 4nl/larva in the Cuvier duct of anesthetized larvae 2dpf;
- After injection put larvae in egg water at 35°C;
- At 2h post injection, check fluorescence microscope the microinjected larvae, eliminating larvae with false positive;
- Keep larvae at 35°C for 3-5 days af microinjection and check the percentage of invaded cells.

Larvae manipulation for inflammation assay and macrophage polarization visualization

To evaluate the role of iron in guiding macrophage polarization, *mpeg1*:cherryF; *tnfa*:eGFP eggs 1dpf were dechorionated (30 for each group) and treated with FAC 100 μM, DFO 100 μM (iron chelator) in a 6 wells plate for 24h. Caudal fin amputation was performed on 3 dpf larvae as described in Pase et al. (2012). The caudal fin was transected with a sterile scalpel, posterior to muscle and notochord under anaesthesia with 0.016% Tricaine (ethyl 3-aminobenzoate, Sigma Aldrich, France) in zebrafish water.

Statistic analysis

The data are expressed as mean ± SD. Statistical analysis was carried out by paired Student's t-test, ANOVA test or Mann-Whitney test. For correlation analysis, the Pearson’s correlation was

assessed. A p value <0.05 was considered to indicate a statistically significant difference between experimental and control groups.

Results

Chapter 1
HDAC6 enzymatic activity inhibition in Multiple Myeloma

1.1 Proliferation and autophagy induction in myeloma cells

The role of HDAC6 in multiple myeloma cells was investigated through its enzymatic activity inhibition by tubacin. Gene expression analysis of HDAC6 was carried out in U266 sensitive (U266 S) and U266 resistant to bortezomib (U266 R) cell lines. Results revealed a significant upregulation of HDAC6 gene in U266 R compared to U266 S (**$p<0.001$) [fig. 5A]. Concerning the role of HDAC6 in cancer cell proliferation, it was evaluated its ability to reduce myeloma cells viability, using tubacin (as HDAC6 enzymatic activity inhibitor) alone and in combination with bortezomib. Both U266 S and U266 R cell lines were treated with tubacin 5 μM, BTZ 15 nM alone and in combination for 24h. Data showed that tubacin did not able to reduce myeloma cells proliferation alone or in combination with bortezomib. In U266 S we observed a significant reduction of cells proliferation only in BTZ-treated cells compared to untreated group. Treatment with tubacin was performed to evaluate if it was able to sensitize U266 R to bortezomib treatment reducing autophagy mechanism in myeloma cells. Data showed that tubacin did not affect U266R proliferation nether alone nor in combination with BTZ compared to untreated cells [fig. 5B].

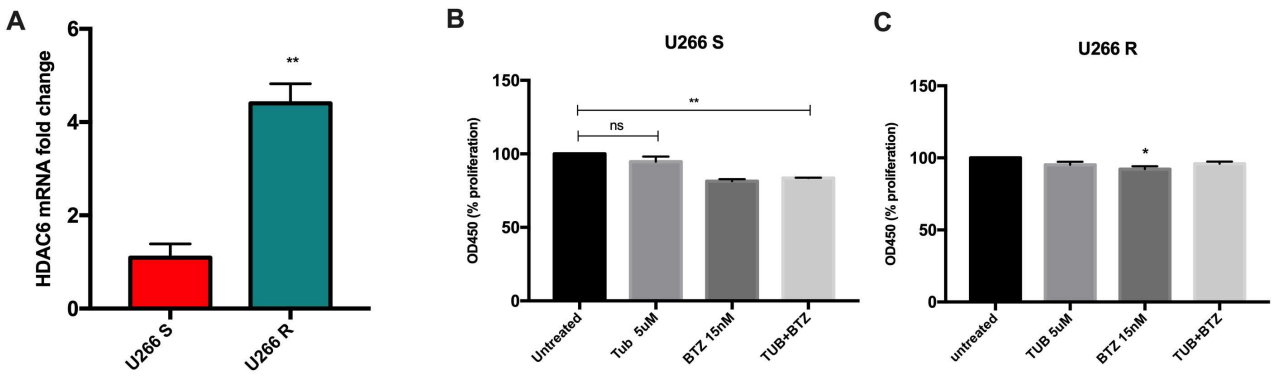

Fig. 5: HDAC6 enzymatic activity inhibition did not exert synergistic effects in myeloma cells. **A.** Higher levels of HDAC6 gene expression in U266 R were founded compared to U266 S at basal conditions. HDAC6 (Histone Deacetylase 6); (**p<0.001). **B.** HDAC6 enzymatic activity inhibition with Tubacin 5uM did not show synergistic effects with bortezomib 15nM in U266 S cells; while BTZ treatment induced reduction of proliferation, co-admnistration of TUB and BTZ did not bortezomib efficacy. **C.** In U266 R of the percentage of myeloma cells survival after tubacin treatment did not change, nether alone nor in combination with bortezomib treatment. HDAC6 inhibition did not sensitize U266 R to bortezomib treatment (*p<0,01; **p<0.001).

Concerning the role of HDAC6 enzymatic activity in autophagy induction, myeloma cells were treated with tubacin 5uM alone or in combination with BTZ 15nM for 24h and autophagolysosomes production was evaluate by FACS analysis (AVO-test). Results proved that autophagy induction by bortezomib treatment in U266 clone was not reduced significantly when tubacin was added in combination with BTZ compared to BTZ-treated group in which it was possible to observe a significant increased percentage (**p<0.002) of autophagy induction compared to untreated cells [fig. 6]. Avo-test and FACS analysis were carried out also in U266R cells with the same experimental conditions, but results did not show any interesting or significant data.

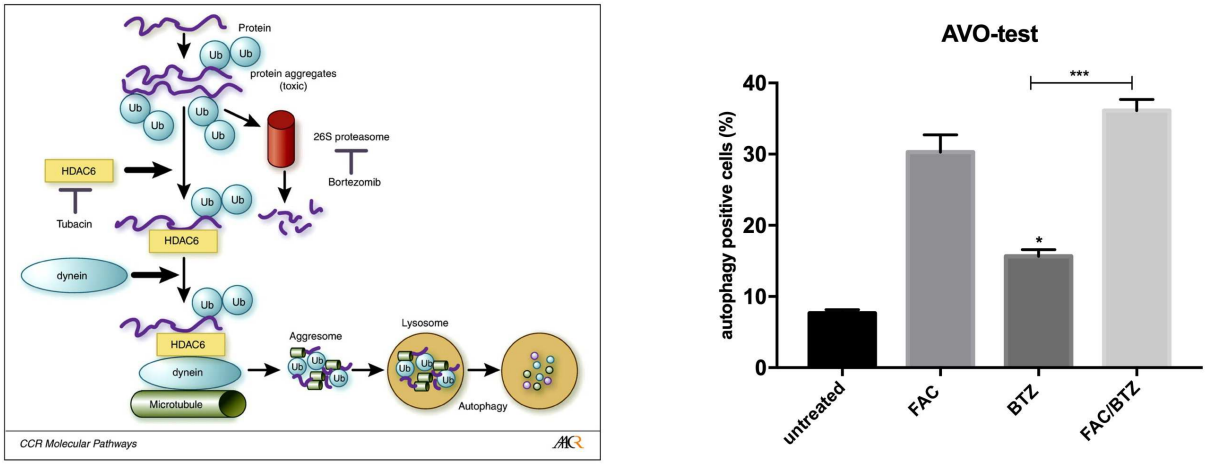

Fig. 6: Percentage of autophagolysosomes vesicles formation analysis by FACS. Schematic view of HDAC6 role in autophagy induction (left). In myeloma cells, autophagy evaluation after 24 h of BTZ and TUB treatment, alone or in combination, showed that autophagy induction by bortezomib treatment (**p<0.002) was not significantly reduced when HDAC6 enzymatic activity was inhibited by Tubacin treatment in combination with BTZ.

1.2 HDAC6 role in regulation of immunosuppressive markers in myeloma cells

Since Keremu et al. demonstrated the existing link in HDAC6 enzymatic activity and expression of some immunosuppressive genes like PD-L1 (Programmed Death-Ligand 1). Interstingly, gene expression analysis by qPCR revealed that U266 R cells show a significantly increase of PD-L1 (***$p<0.001$) and IL-10 (*$p<0.01$) levels compared to U266 S cells [fig. 7A]. Increased levels of PD-L1 in U266 R cells compared to U266 clone were also confirmed by FACS analysis [fig.7B]. We also investigated the role of HDAC6 in regulation of immune-modulatory markers expressed by myeloma cells. To evaluate if HDAC6 could be involved in regulation of PD-L1 or IL-10 immunosuppressive markers, U266 S and U266 R cells were treated with tubacin 5uM for 24h and gene expression of PD-L1 and IL-10 was carried out. Data proved that enzymatic activity inhibition of HDAC6 with tubacin in U266 S cell determined a significant reduction of gene expression levels of both PD-L1 (**$p<0.001$) and IL-10 (*$p<0.05$) compared to control group. Interestingly, HDAC6 enzymatic activity inhibition by tubacin treatment was able to downregulate PD-L1 (**$p<0,001$) and IL-10 (***$p<0,0001$) expression also in U266 R cells [fig.7C].

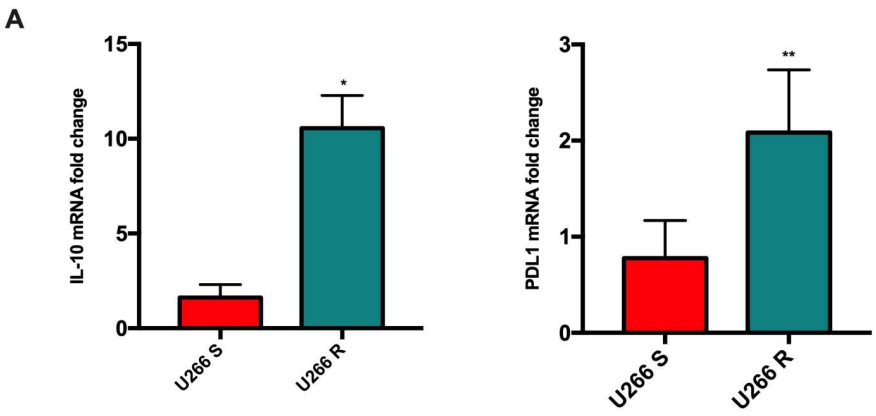
A
IL-10 mRNA fold change
15
10
5
0
*
U266 S
U266 R
PDL1 mRNA fold change
3
2
1
0
**
U266 S
U266 R

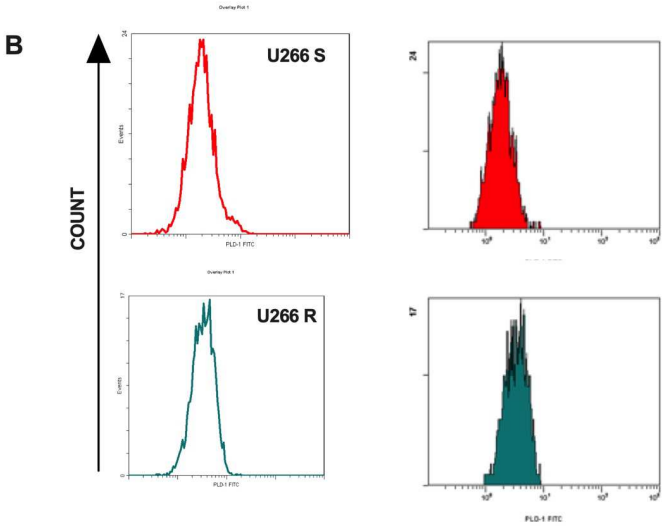
B
COUNT
U266 S
U266 R
PLD-1 FITC

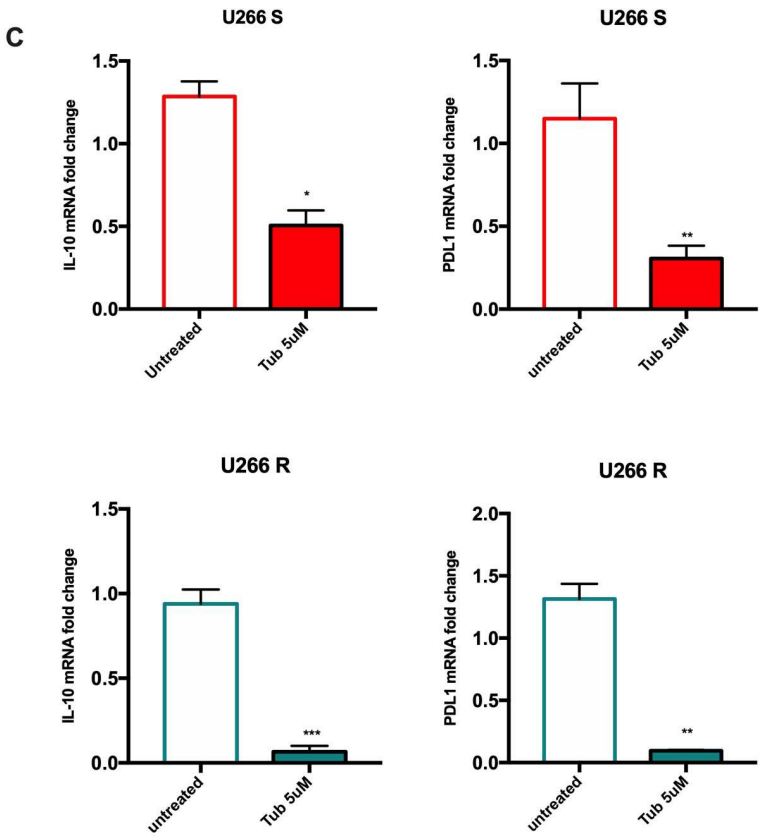
C
U266 S
IL-10 mRNA fold change
1.5
1.0
0.5
0.0
*
Untreated
Tub 5uM
U266 S
PDL1 mRNA fold change
1.5
1.0
0.5
0.0
**
untreated
Tub 5uM
U266 R
IL-10 mRNA fold change
1.5
1.0
0.5
0.0
***
untreated
Tub 5uM
U266 R
PDL1 mRNA fold change
2.0
1.5
1.0
0.5
0.0
**
untreated
Tub 5uM

Fig. 7: HDAC6 modulates gene expression of some immune-stimulatory markers in myeloma cells.

Myeloma resistant cells (U266R) showed increased levels of PD-L1 and IL-10 when compared to U266 sensitive cells, at basal conditions (*$p<0.05$; **$p<0.001$***$p<0.0001$). FACS analysis of PD-L1 in myeloma cells confirmed gene expression analysis. It was observed increased levels of PD-L1 in U266 R compared to sensitive clone (Results are showed as FMI) **[A**; **B].** HDAC6 enzymatic activity inhibition with tubacin 5uM for 24h resulted in PD-L1 and IL-10 downregulation in U266 S and U266 R cell lines. PD-L1 (Programmed Death-Ligand 1); IL-10 (Interleukin-10) **[C]**.

Both U266 S and U266 R cells were treated with tubacin up to 3h and levels of STAT3 phosphorylation (pSTAT3) were measured by FACS analysis. Results proved that U266 R did not show a significant change of pSTAT3 compared to U266 S at basal conditions (U266 S= 5,46%; U266 R= 4.49%). Interstingly, tubacin treatment was able to reduce the percentage of pSTAT3 in both cell lines after 1h of its administration. In particular, the percentage of pSTAT3 in U266 S tubacin 5uM treated was 2.43% compared to 5.46% of untreated cells. U266 R cells revealed a reduction of percentage from 4.49% for the control group to 0.92% for the tubacin treated cells [fig. 8A]. Stimulation with Il-6 100ng/ml was used as positive control, since IL-6 induce pSTAT3. Data highlighted that myeloma cells in which were co-treated IL-16 and Tubacin 5uM the percentage of pSTAT3 was reduced (10.54%) compared to cells IL-6 treated (20.03%) (right) [fig. 8B].

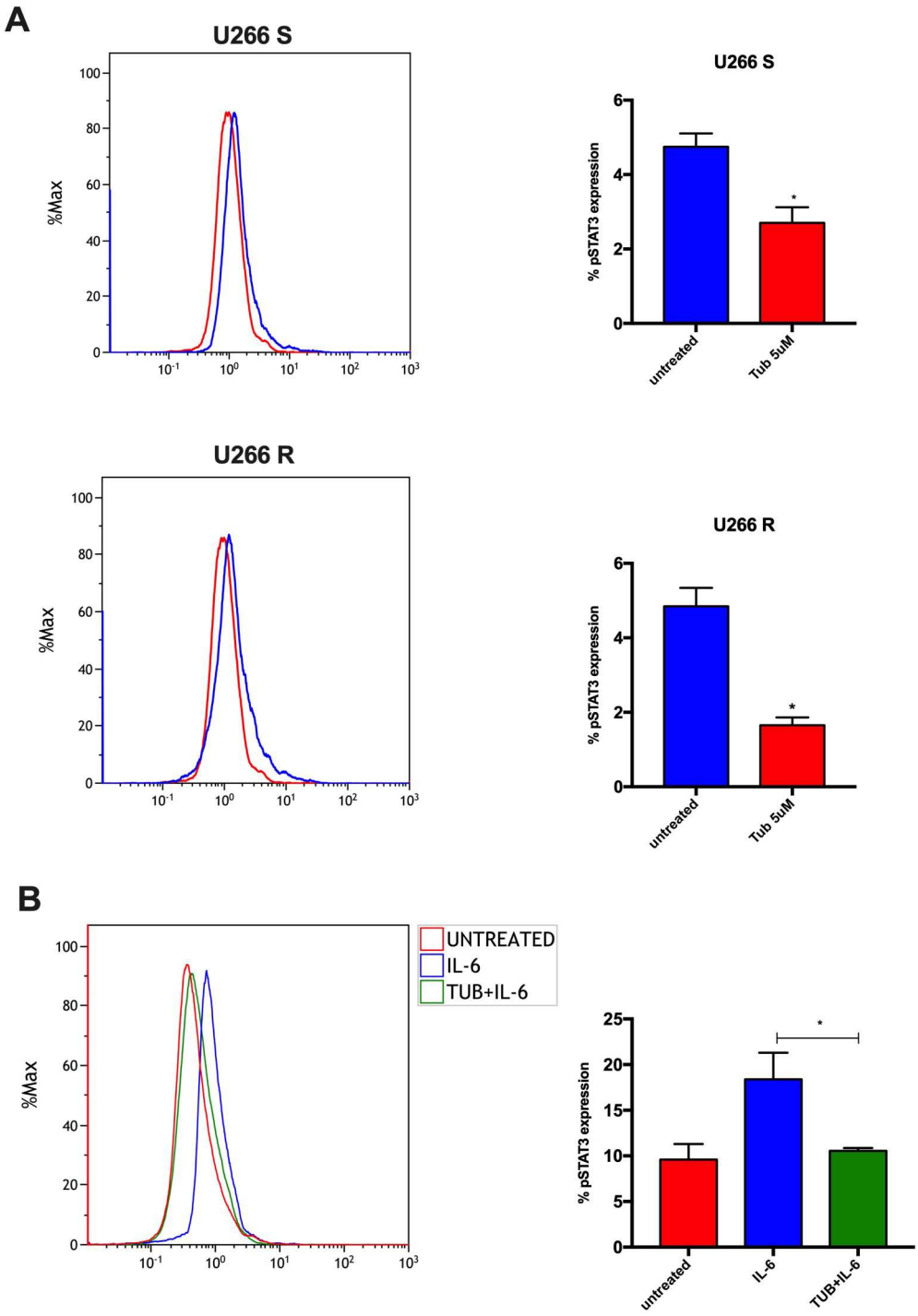

Fig. 8: HDAC6 promotes pSTAT3 activation in myeloma model. FACS analysis of pSTAT3 in myeloma cells. even if U266 S and U266 R did not show any significant difference in pSTAT3 levels at basal conditions, tubacin treatment at several timepoints, revealed a significant reduction in pSTAT3 levels after 1h of its administration in U266 S (2.45%) and U266 (0.92%) R cells (**A**). Positive control by IL-6 100 ng/ul treatment was used to evaluate pSTAT3 induction (**B**). (Figure shows representative data from one experiment). IL-6 (interleukin-6); TUB (Tubacin 5uM).

Chapter2

Iron as key player on inducing myeloma cell resistance to bortezomib

2.1 Iron treatment improves Myeloma cells energetic metabolism promoting bortezomib resistance.

2.1.1 Myeloma cells are able to internalize iron

U266 R cells showed higher expression levels of the main genes involved in iron trafficking as FPN(**p<0.001), DMT-1 (*p<0.01) and TFRC1 (**p<0.001) compared to U266 S at basal conditions [fig. 9].

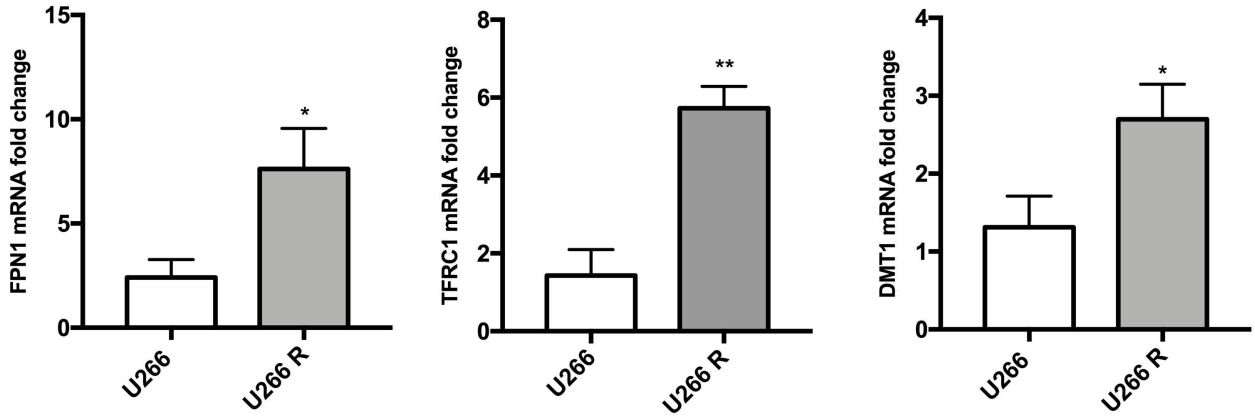

Fig. 9: **U266 R showed higher levels of iron trafficking markers than U266S**. Gene expression analysis revealed increased levels of iron trafficking genes as FPN, DMT-1 and TFRC1 in U266 resistant cells (U266R) compared to U266 sensitive cells (U266 S), at basal conditions. 2^-ΔΔCt calculated value in control was 1. (* p<0.01; *p<.001); **p<0.001). FPN (Ferroportin); DMT-1 (Divalent Metal Transporter 1); TFRC1 (Transferrin receptor 1).

Excess of iron lead to LIP (labile iron pool) formation that are vescicles in which cells store reactive iron. Reactive and free iron is able to induce Fenton reaction and then ROS production. To confirm iron intake in myeloma cells and their ability to uptake iron as LIP, FACS analysis was carried out in U266 treated with FAC 400uM. Data showed a significant increase of LIP formation when myeloma cels were treated with FAC ($p= 0.001$) compared to the control group [fig.10 A]. Also, it has been evaluated gene expression of genes involved in iron trafficking. Results showed a significant upregulation of the iron importer DMT-1 and iron exporter FPN in myeloma cell lines after 6h and 24h of iron treatment [fig. 10B]. In addiction, apoptosis myeloma cells (U266, OPM2, H929) was carried out after 24h of with FAC 400 μM treatment by FACS analysis. Results did not show any significant difference in cell viability comparing myeloma cells FAC-treated to untreated cells [fi. 10 C].

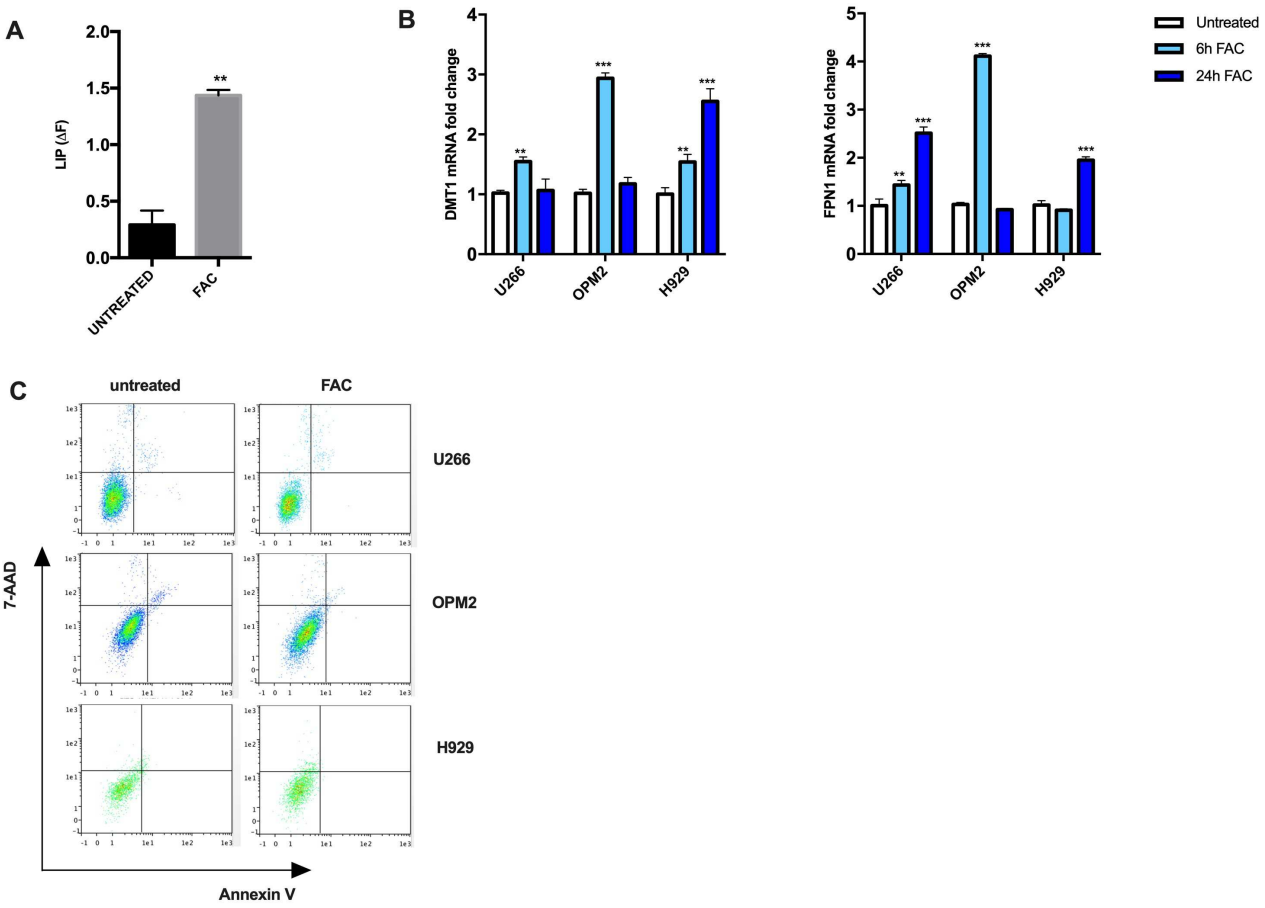

Fig.10: Iron treatment did not affect myeloma cells viability. **A.** Flow cytometry analysis of LIP (Labile Iron Pool) in myeloma cells expressed as ΔF (variation of mean fluorescence intensity) ; **p<0.001. **B.** FAC treatment up to 24h induced gene expression of iron trafficking markers as FPN1 and DMT1 in myeloma cells. Calculated value of 2^-ΔΔCt in untreated myeloma cells was 1 (*p<0,1; **p<0.001; ***p<0.0001). FPN (Ferroportin1);DMT1 (Divalent Tranporter 1). **C.** Apoptosis of myeloma cell lines (U266, OPM2, H929) was carried out after 24h of FAC 400uM treatment by flow cytometry analysis. (Figure shows representative data from one experiment).

2.1.2. Iron modifies the redox status of myeloma cells improving their energetic metabolism.

High levels of ROS production in cancer cells is due to their high rate of proliferation and cell instability. We observed that FAC 400 μM treatment of myeloma cells (U266, OPM2, H929) was able to induce ROS production with a pick to 30 minutes (U266, OPM2 ***$p<0.0001$; H929 *$p<0.01$) [Fig. 11A]. Cells were able to response to the oxidative stress inducing activation of scavenger molecules as GLUT-S-TRANSFERASE, HMOX-1, SOD2 and CYTB gene expression after 30 minutes of FAC treatment compared to untreated cells [fig. 11B].

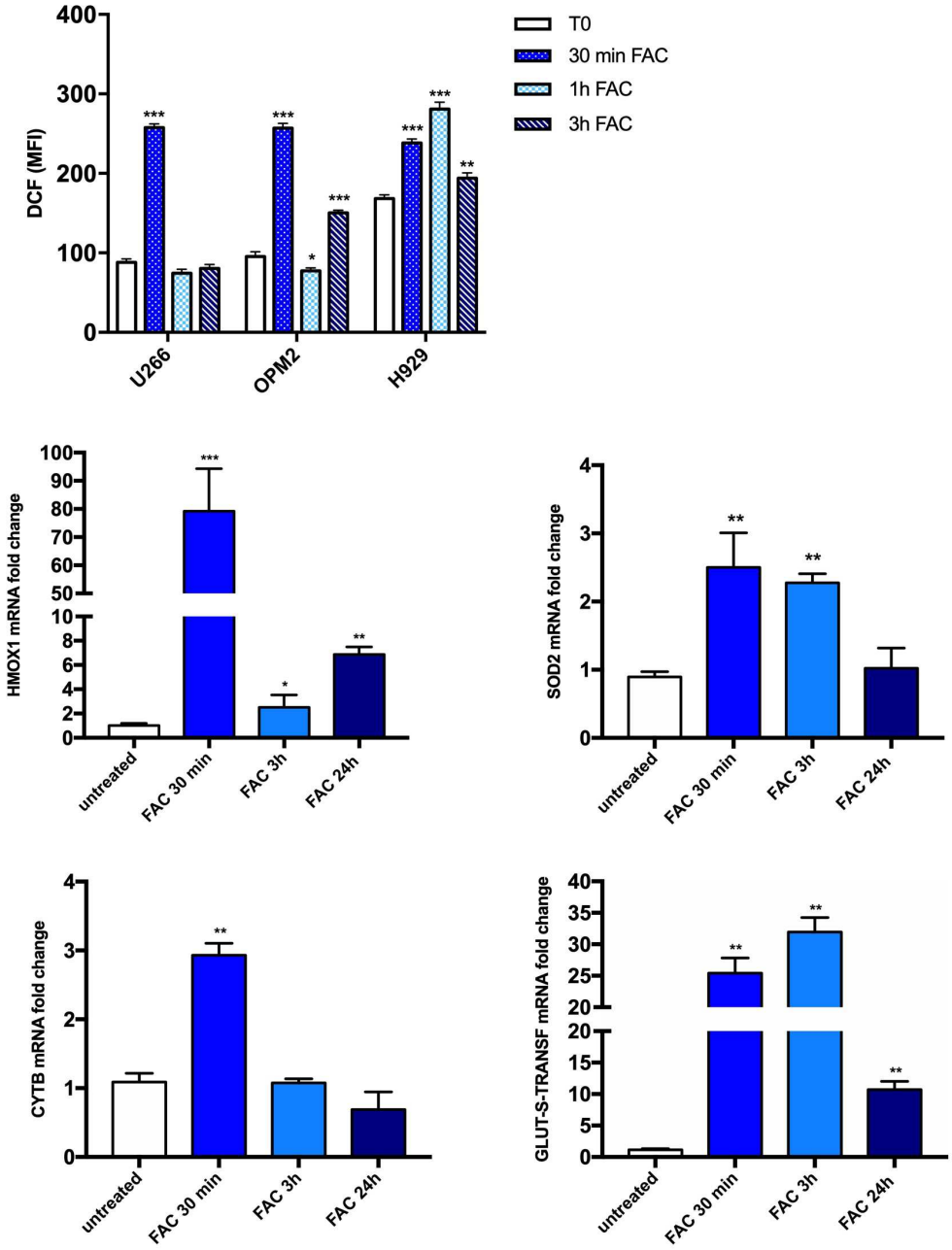

Fig. 11: **Iron induced oxidative stress in myeloma cells. A.** Reactive oxygen species (ROS) were measured in myeloma cell lines (U266, OPM2, H929) at several timepoints up to 3h, after FAC 400uM treatment. Results are showed as MFI (mean fluorescence intensity); *p<0.01, ***p<0.0001. **B**. gene expression analysis of GLUT-S (glutathione-s-transferase), HMOX1(Heme Oxygenase 1), CYTB (Cytocrome B), SOD2 (Superoxyde dismutase 2), as markers of oxidative stress, in myeloma cells after FAC administration. Calculated value of 2^-ΔΔCt in untreated myeloma cells was 1 (**p<0,001).

Since iron is an essential component of both mitochondrial function and OXPHOS, it was evaluated if iron could modify myeloma cells response to bortezomib treatment improving the mitochondrial fitness. Our data showed that treatment with FAC improved mithocondria functions. Interestingly, FACS analysis of mitochondrial membrane potential status with DiOC(2)3 showed a reduction of mitochondrial membrane potencial after 6h of iron addition Cells were able to restore their mitochodrial membrane potential after 24h of treatment (**p<0.001; ***p<0.001), as confirmed with the increase of mitochondrial mass at the same timepoint by FACS analysis with MitoTracker Probe [fig. 11A]. Finally, qPCR analysis showed that myeloma cells modify their mitochondrial functions also upregulating some genes involved in mitochondrial biogenesis and energetic metabolism. In particular, after 30 minutes of iron addition, we observed a significant upregulation of TFAM (***p<0.001) ND4 (***p<0.0001) as mitochondrial biogenesis markers [fig.11B].

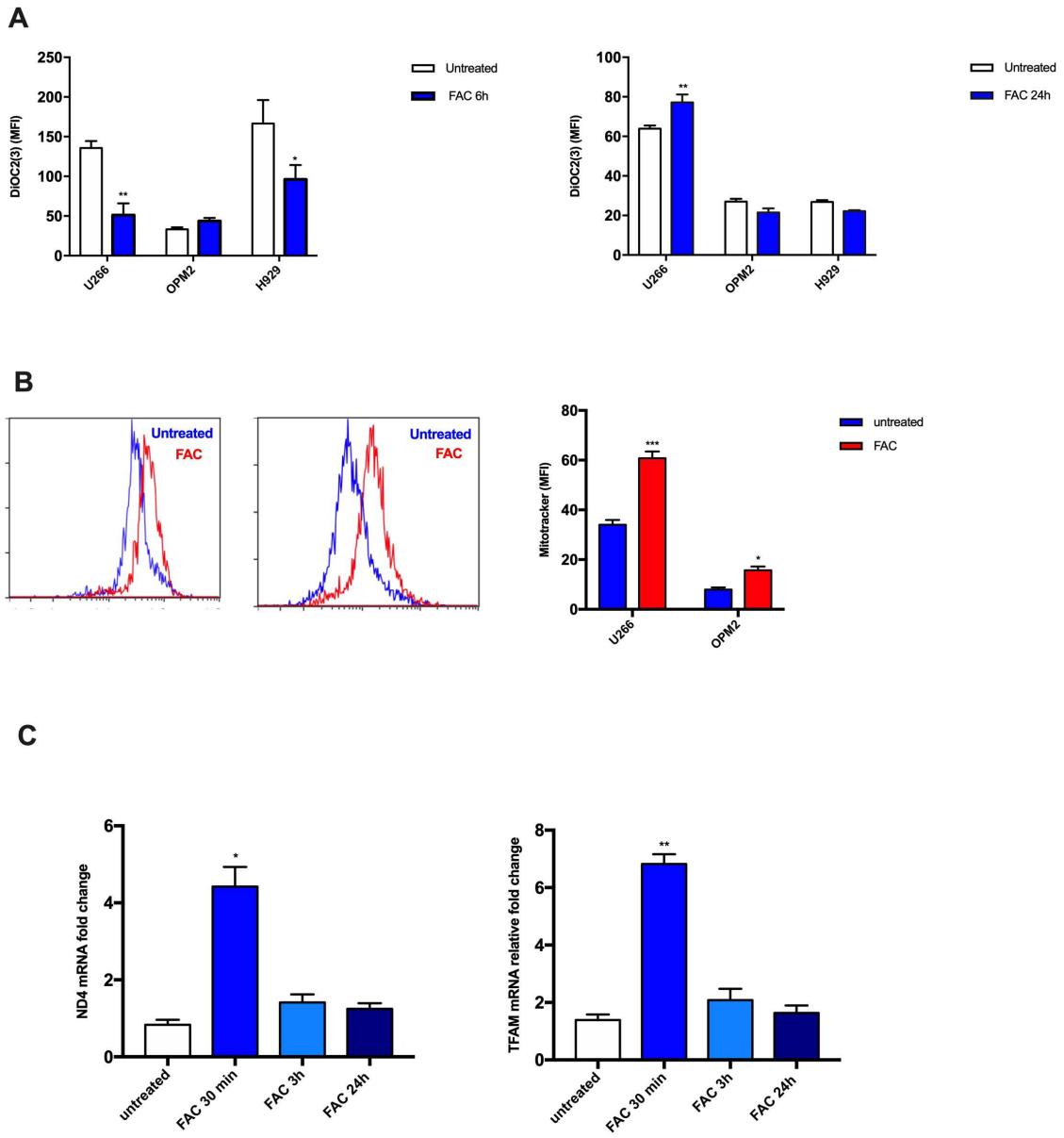

Fig. 12: Iron treatment improved mitochondrial fitness in myeloma cells. Flow cytometry analysis of mitochondrial membrane depolarization with DiOC (2)3 expressed as MFI (mean fluorescence intensity) in myeloma cells treated with FAC up to 24h (**A**). Evaluation of mitochondrial mass in myeloma cells with MitoTracker Probe by FACS. Resulted were expressed as MFI. Flow cytometry plot shows representative data from one experiment (**B**). **p<0.001; ***p<0.0001. Gene expression analysis by qPCR of mitochondrial fitness markers was carried out after FAC treatment at several timepoints in U266 S, as representative m odel. ND4 (NADH-ubiquinone oxidoreductase chain 4), TFAM (Mitochondrial Transcription Factor 1) gene expression levels were evaluated. Calculated value of 2^-ΔΔCt in untreated myeloma cells was 1. **p<0.001; ***p<0.0001. (**C**).

2.1.3 Iron induces autophagy as protective mechanism in myeloma cells.

Recently, it has been reported that myeloma cells activate autophagy as strategy to elude proteotoxic inducing myeloma cells resistance. We evaluated autophagy activation as mechanism of resistance induced by iron. H929-LC3-GFP-mCherry cells were treated with FAC for 24h to prove LC3II activation as main marker of autophagy induction. Immunofluorescence allow us to observe increased autophagy after FAC treatment (yellow puncta) compared to untreated cells. Bafilomycin was used as positive control to induce autophagic flux [fig. 13]

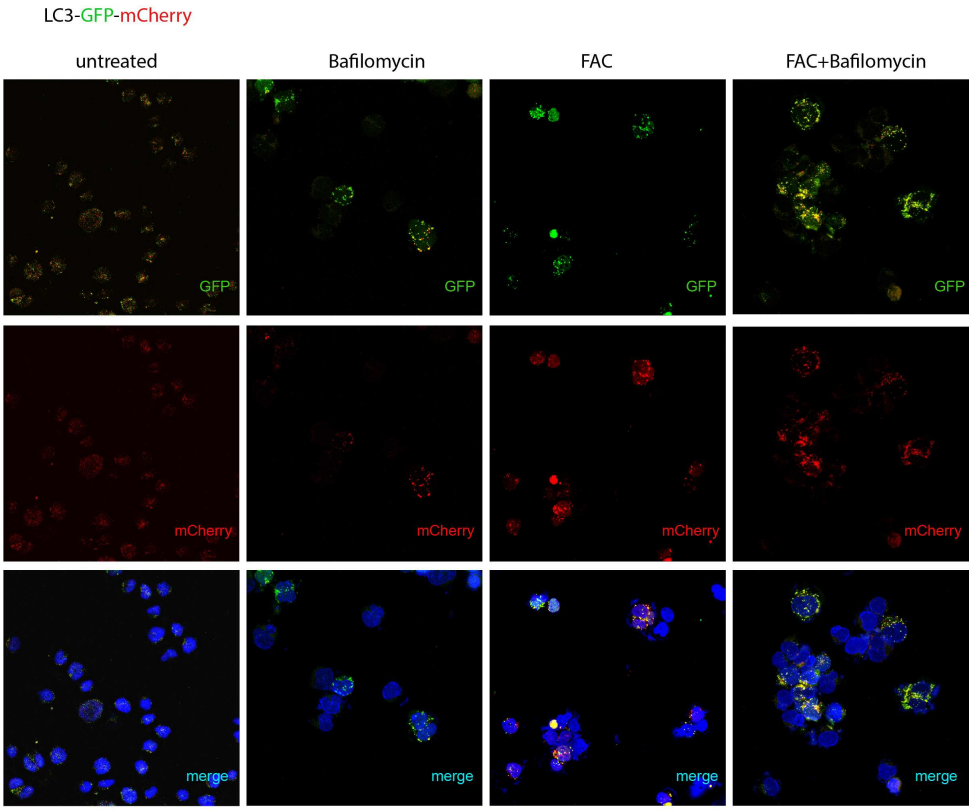

Fig. 13: Iron induces autophagy in myeloma cells. Detection of LC3II activation after FAC treatment was performed by incubation H929 -GFP-cherry cell line. Counterstaining of cells was performed by using the nuclear dye, DAPI (blue). Bafylomicin was used as positive control to inhibit lysosomal degradation thus reflecting the amount of LC3II.

2.1.4. Iron induce bortezomib resistance in myeloma cells.

Improved mitochondrial fitness has been demonstrated to be linked to drug resistance in some solid tumor types. U266 FAC-pretreated (U266-Fe) showed resistance to bortezomib treatment since their rate of proliferation did not change compared to the control group. Since iron modify energetic metabolism in U266-Fe upregulating mitochondrial biogenesis and energetic metabolism markers compared U266 S, evaluation of myeloma cells response to bortezomib treatment was carried out. Analysis of cell viability revealed that U266-Fe showed reduced percentage of apoptotic cellsv after BTZ treatment compared to U266 S, in which BTZ treatment significantly affect cell viability. Interestingly, to confirm the ability of iron in inducing BTZ resistance in myeloma cells, U266-Fe were co-treated with FAC 400uM and the iron chelator Deferasirox (DFX) 50uM for 24h. Bortezomib was added for 24h and cell proliferation was evaluated. Data showed that iron chelation in U266-Fe cells sensitized myeloma cells to BTZ treatment ($p<0.001$) compared to U266-Fe BTZ treated [fig. 14].

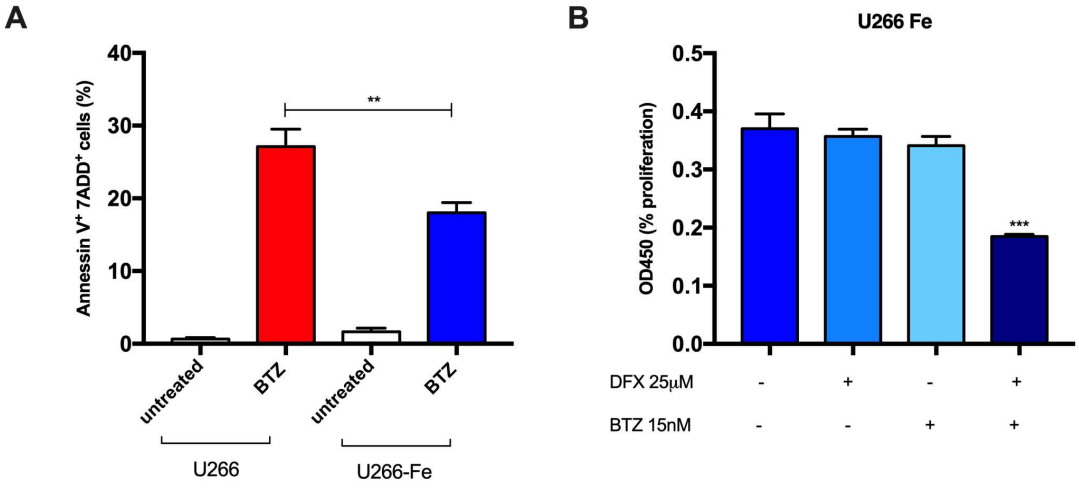

Fig.14: iron reduces apoptosis of myeloma cells induced by bortezomib. A. apoptosis evaluation by flow cytometry in U266 and U266-Fe (FAC pre-treated) after BTZ 15 nM administration for 24h. (**$p<0.001$). **B.** U266 cells (U266-Fe) were co-treated with FAC 400uM and DFX (deferasirox, iron chelator) for 24h. BTZ 15nM was administrated for 24h and cell viability was measured by XTT assay; **$p<0.001$.

Data highlighted that bortezomib treatment affected mitochondrial fintness in U266 S. Results proved that increase of ROS production (1h: **p<0.001; 3h: ***p<0.0001) after BTZ treatment up to 3h [fig.15A] was accomplished to the downregulation of energetic matebolism related genes (ND4 and CYTB) in U266 S cells [Fig. 15B], whereas U266-Fe did not show any significant variation in ROS production and expression levels of the same genes after BTZ treatment compared to untreated cells.

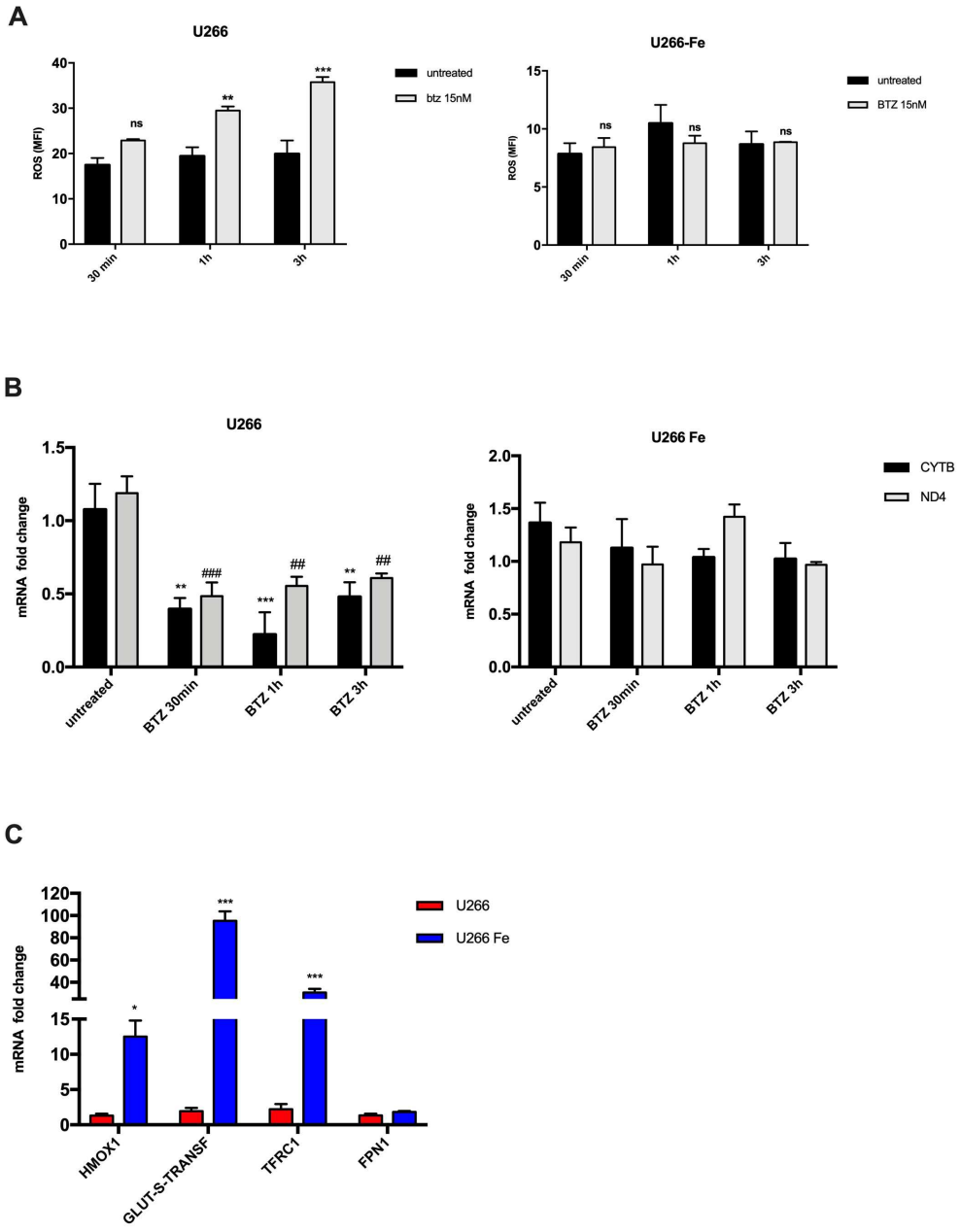

Fig. 15: iron improves mitochondrial activity in myeloma cells protecting against toxic effects induced by bortezomib. A. U266 and U266-Fe were treated with BTZ up to 3h. Reactive oxygen species (ROS) production was measured by flow cytometry; resulted were expressed as MFI (mean fluorescence intensity). **B:** gene expression analysis of energetic metabolism markers was evaluated at several timepoints up to 3h. Calculated value of 2^-ΔΔCt in untreated myeloma cells was 1. ND4 (NADH-ubiquinone oxidoreductase chain 4), CYTB (Cytocrome B). **p<0.001; ***p<0.0001.

2.1.5. Iron induces in vivo bortezomib resistance of myeloma cells

To convalidate the role of iron in bortezomib resistance induced in myeloma cells, we used Zebrafish as animal model. Zebrafish *mfap4:tomato* mutant larvae 2dpf were used to xenotransplantate U266 S and U266-Fe. All myeloma cells were xenotransplantated in the Cuvier duct. Injected larvae were subsequently treated with BTZ 15nM up to 48h. Analysis of myeloma cells in the CHT (Caudal Hemapotietic Tissue) revealed a significant reduction (***$p<0.001$) of U266 S in larvae BTZ treated compared to untreated ones, at 48h [fig. 16A]. On the other hand, analysis of U266-Fe in the CHT of larvae BTZ treated, even if showed small sensitivity (*$p<0.05$) of myeloma cells in CHT after 24h of BTZ treatment, it did not evidence a significant reduction of cell number compared to the control group, after 48h [fig.16B].

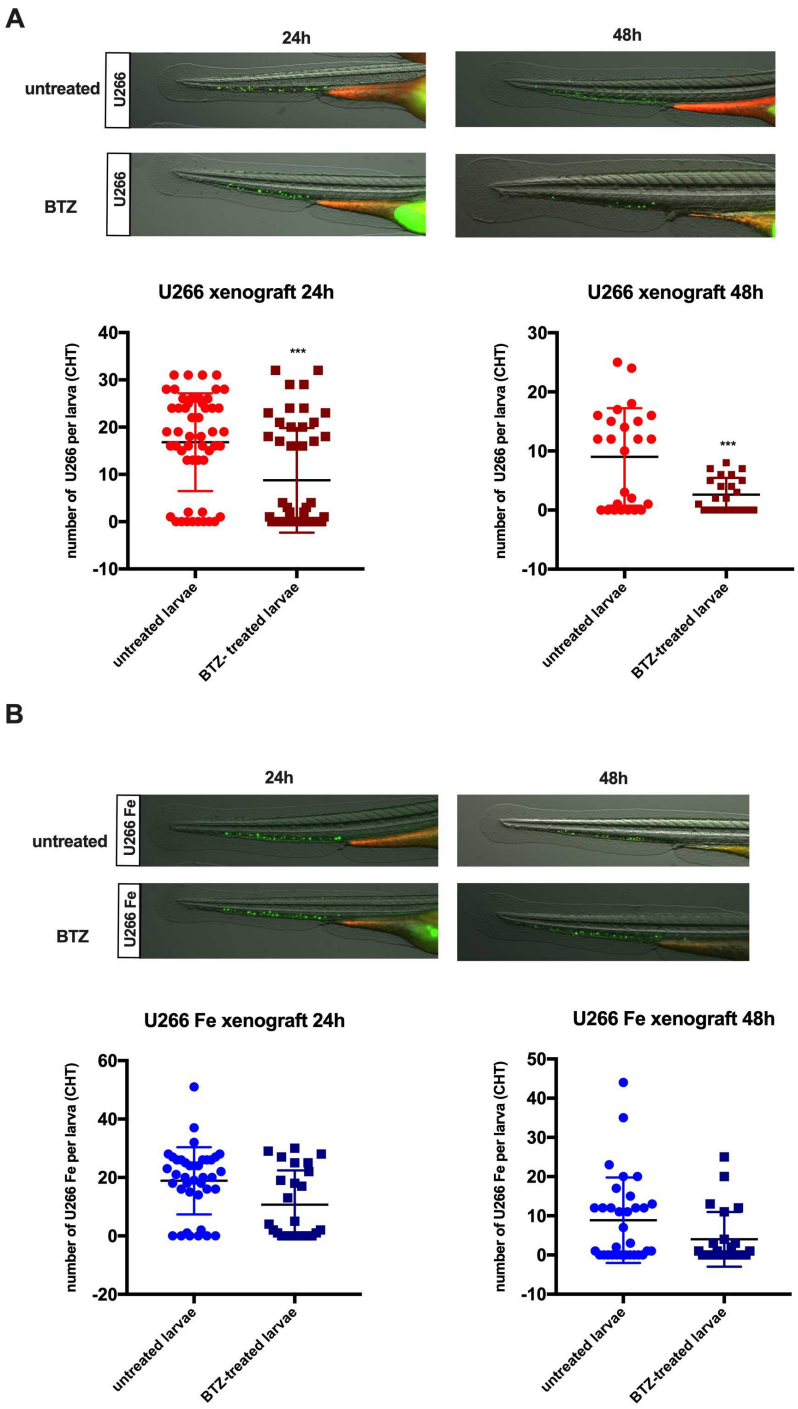

Fig. 16: rion induces *in vivo* bortezomib resistance of myeloma cells. U266 and U266-Fe were labelled with DiO Vybriant stainer (green) and xenotranplantated in zebrafish casper larvae 2dpf. Larve were treated with BTZ 15nM for 48h and MM cells number was counted in CHT at 24h and 48h. **A.** U266 xenotransplantation in zebrafish larvae (left); results are expressed as number of MM cells in the CHT per larva (right). **B.** U266-Fe xenotranplantation in zebrafish larvae (left); results are expressed as number of MM cells in the CHT per larva (right). *p<0.05; ***p<0.0001. MM (Multiple Myeloma); CHT (Caudal Hematopoietic Tissue).

2.2 Iron and tumor macrophages

2.2.1 Iron promotes immuno-suppressive phenotype (M2) in macrophages

We studied the effects of FAC treatment in monocytes cells such as U937 cell line and human primary monocytes cells. U937 cells showed an increase of iron trafficking genes markers (TFRC1 and DMT-1) and upregulation of oxidative stress protein HMOX1 [fig. 17A]. We also treated U937 cells with FAC 100 uM for 24h and apoptosis was evaluated by FACS to prove that iron did not affect macrophages viability. The data showed that cell viability of FAC-treated U937 was similar to untreated group [fig. 17B].

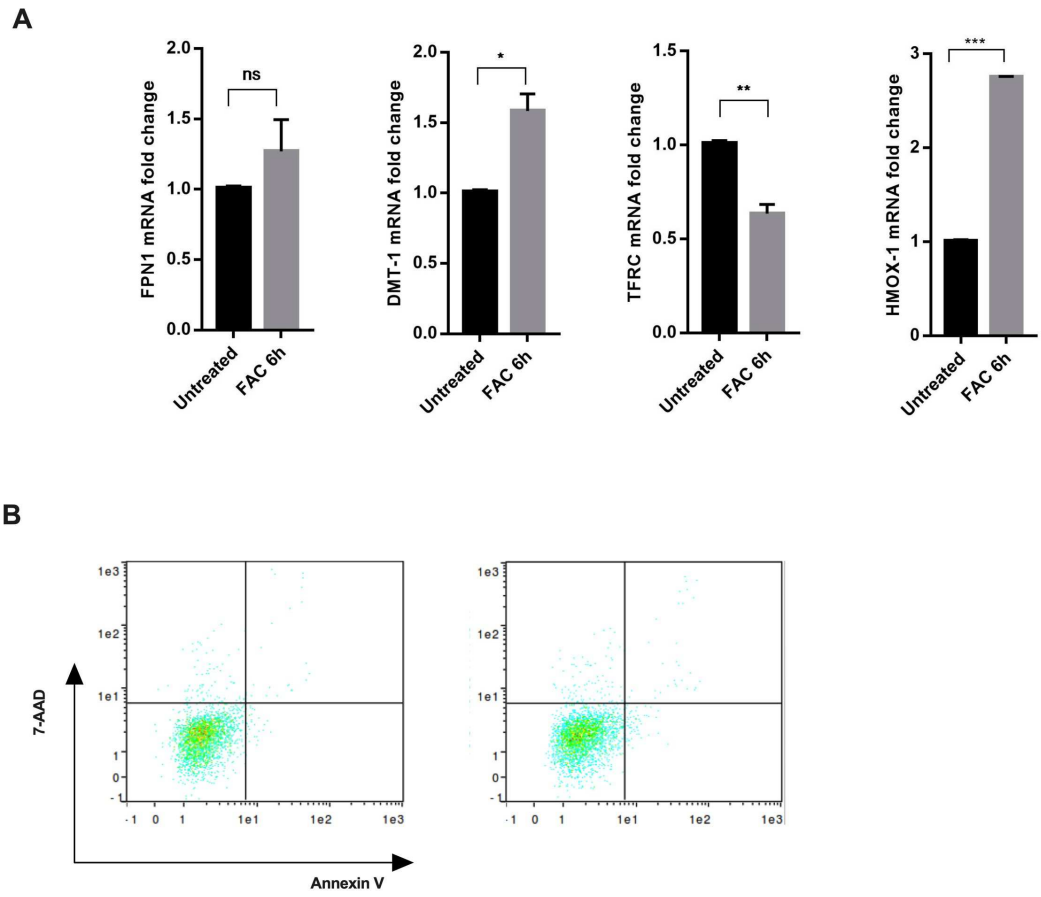

Fig. 17. Iron internalization did not affect monocytes viability. A. Gene expression analysis of iron trafficking markers FPN1 and DMT-1 in U937 treated with FAC up to 6h. Calculated value of 2^-ΔΔCt in untreated U937 cells was 1. FPN-1 (Ferroportin 1); DMT-1 (Divalent Metal Transporter 1) *p<0.01. **B.** U937 cell line was treated with FAC 100uM for 24h. Evaluation apoptosis was carried out by flow cytometry analysis. The figure shows representative data from one experiment.

Macrophages are capable to switch their phenotype in M1 (pro-inflammatory) or M2 (anti-inflammatory) types. Interestingly, FAC treatment executed for 24h in U937 cells showed the anti-inflammatory switch phenotype. In particular, FACS analysis revealed a significant increase of $CD206^+$ and decreased $HLA\text{-}DR^-$ levels compared to untreated cells [fig. 18A]. To confirm FACS data, gene expression analysis of several pro-inflammatory (IL-6, CCL2, TNFa) and anti-inflammatory cytokines (TGFb) were performed. We observed the downregulation of IL-6 (*$p<0.01$), CCL2(**$p<0.001$), TNFa (*$p<0.01$) and the significant upregulation of the anti-inflammatory cytokine TGFb (*$p<0.01$) in monocytes treated with FAC compared to untreated cells.

In addiction, iron treatment was able to increase the mRNA expression of Arginase1(ARG1), as immune suppressive marker [fig. 18B].

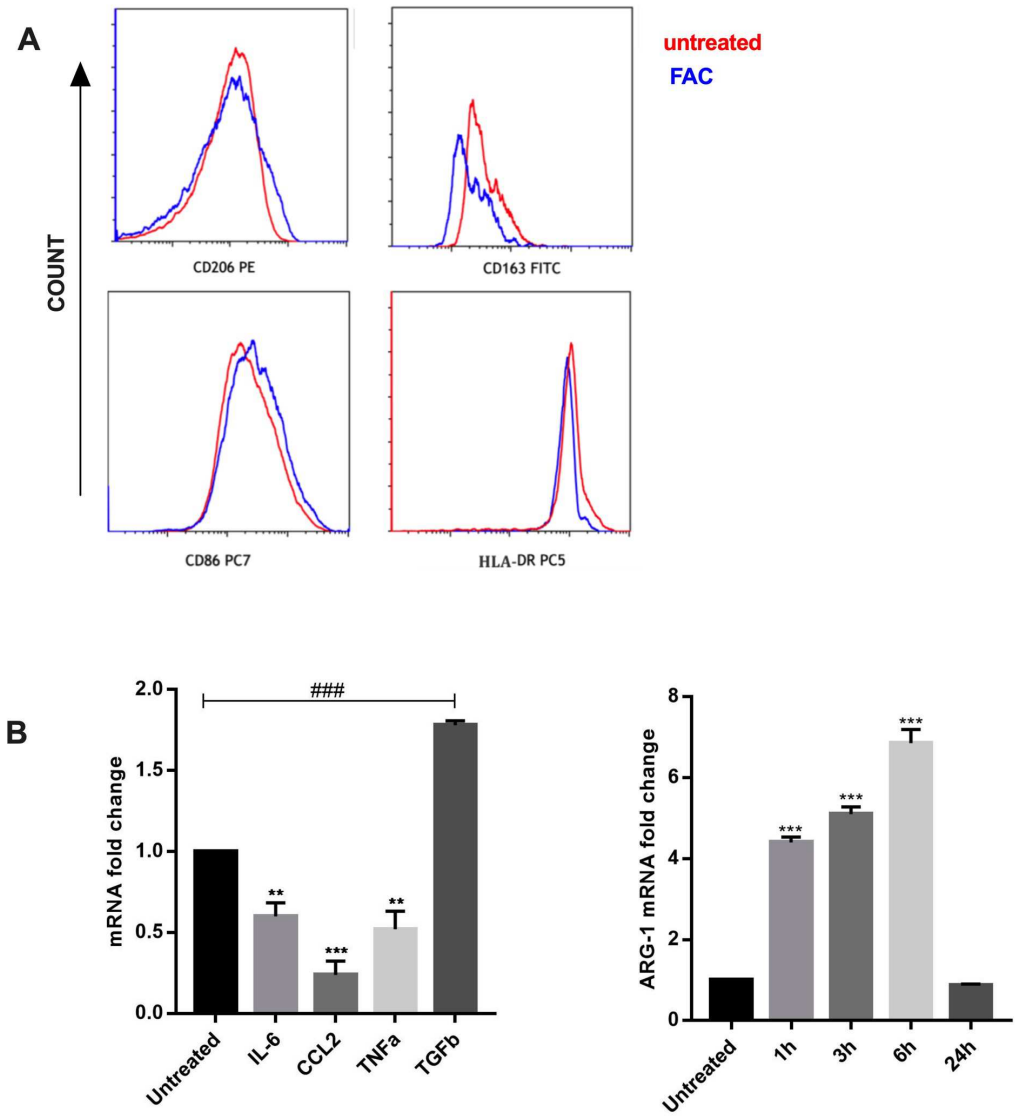

Fig. 18: Iron activates monocytes towards anti-inflammatory phenotype. U937 cells were treated with FAC 100uM up to 48h and activation of anti-inflammatory phenotype was evaluated. **A.** analysis by FACS of several immuno-modulatory markers ($CD206^+$; $CD163^+$; $CD86^+$; $HLA\text{-}DR^-$) in U937 FAC-treated in respect with U937 control. The figure shows representative data from one experiment. **B.** Gene expression analysis of some immune-modulatory factors. Calculated value of 2^-ΔΔCt in untreated U937 cells was 1. IL-6 (Interleukin-6); TNFa (Tumor Necrosis Factor 1); CCL2 (C-C Motif Chemokine Ligand 2); TGFb (Transforming Growth Factor b); ARG-1 (Arginase 1). *p<0.01; ***p<0.0001

Moreover, we performed *ex vivo* experiments. Healthy donor monocytes were seeded and treated with FAC for 24h. Followed, U266 were cultured for 72h with FAC treated monocytes and M2 polarization markers (CD206, HLA-DR) were evaluated by FACS. Results showed higher levels of $CD206^{+}$ in FAC treated monocytes (*p<0.01) compared to untreated when U266 were co-cultured with FAC-treated monocytes. On the other hand, a significant reduction of $HLA\text{-}DR^{-}$ was observed when HD monocytes were treated with FAC alone (*p<0.01) or in co-colture with U266 (**p<0.001) [fig. 19].

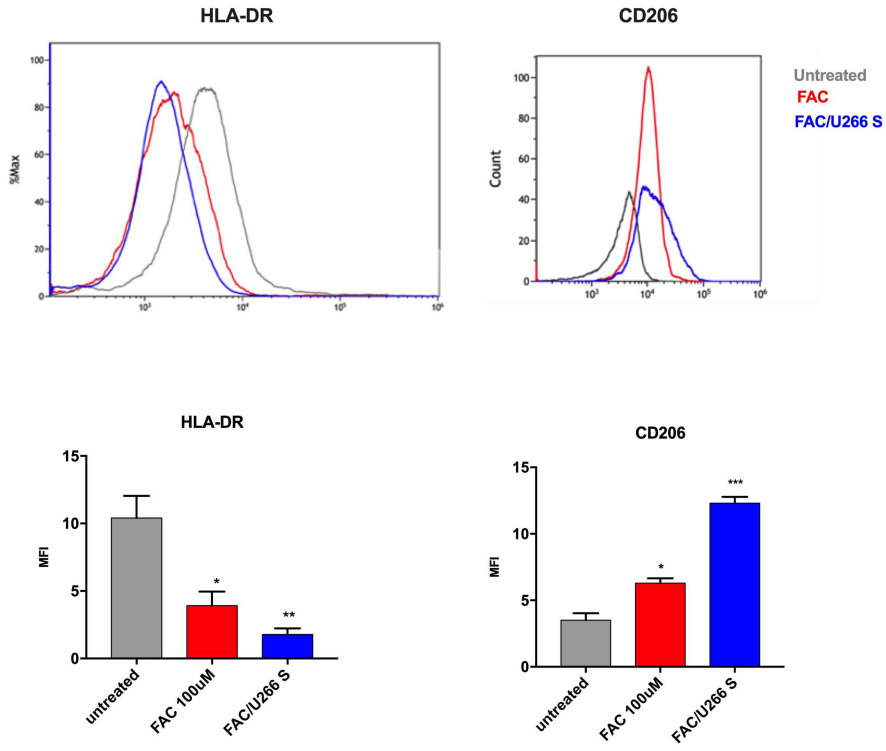

Fig. 19: Iron promotes anti-inflammatory phenotype in primary monocyte cultures. HD monocytes were treated with FAC 100uM for 24 and then co-coltured with U266 cells. Evaluation of immune-modulatory markers ($CD206^{+}$, $HLA\text{-}DR^{-}$) was executed by flow cytometry. The plot shows representative data from one experiment. HD (healthy donor) Untreated (untreated monocytes); FAC (iron treated monocytes); FAC/U266S (monocytes FAC treated co-coltured with U266 cells). *p<0.01; **p<0.001; ***p<0.0001

2.2.2 FAC-induced TAMs promote bortezomib resistance in myeloma cells

It has been demonstrated that tumor associated macrophages (TAMs) promote cancer resistance through releasing iron in tumor macroenvironment, cancer cells uptake iron modifying their energetic metabolism and, finally, developing drug resistance. We investigated the ability of macrophages to release iron thus favoring myeloma cell resistance. HD monocytes were treated with iron. After 24h, myeloma cells (U266) were added, co-cultured cells were then treated with BTZ and myeloma cells apoptosis was evaluated [Fig. 20A]. FACs analysis revealed that monocytes treated with FAC were able to proctect U266 to BTZ addiction, compared to untreated monocytes [Fig. 20B]. Interestingly, U266 co-cultured with FAC-treated monocytes showed increased gene expression analysis of mitochondrial biogenesis marker as TFAM. We also observed increased mitochondrial mass in U266 co-cultured with monocytes treated with FAC by Mitotracker FACS analyisis [Fig. 20C].

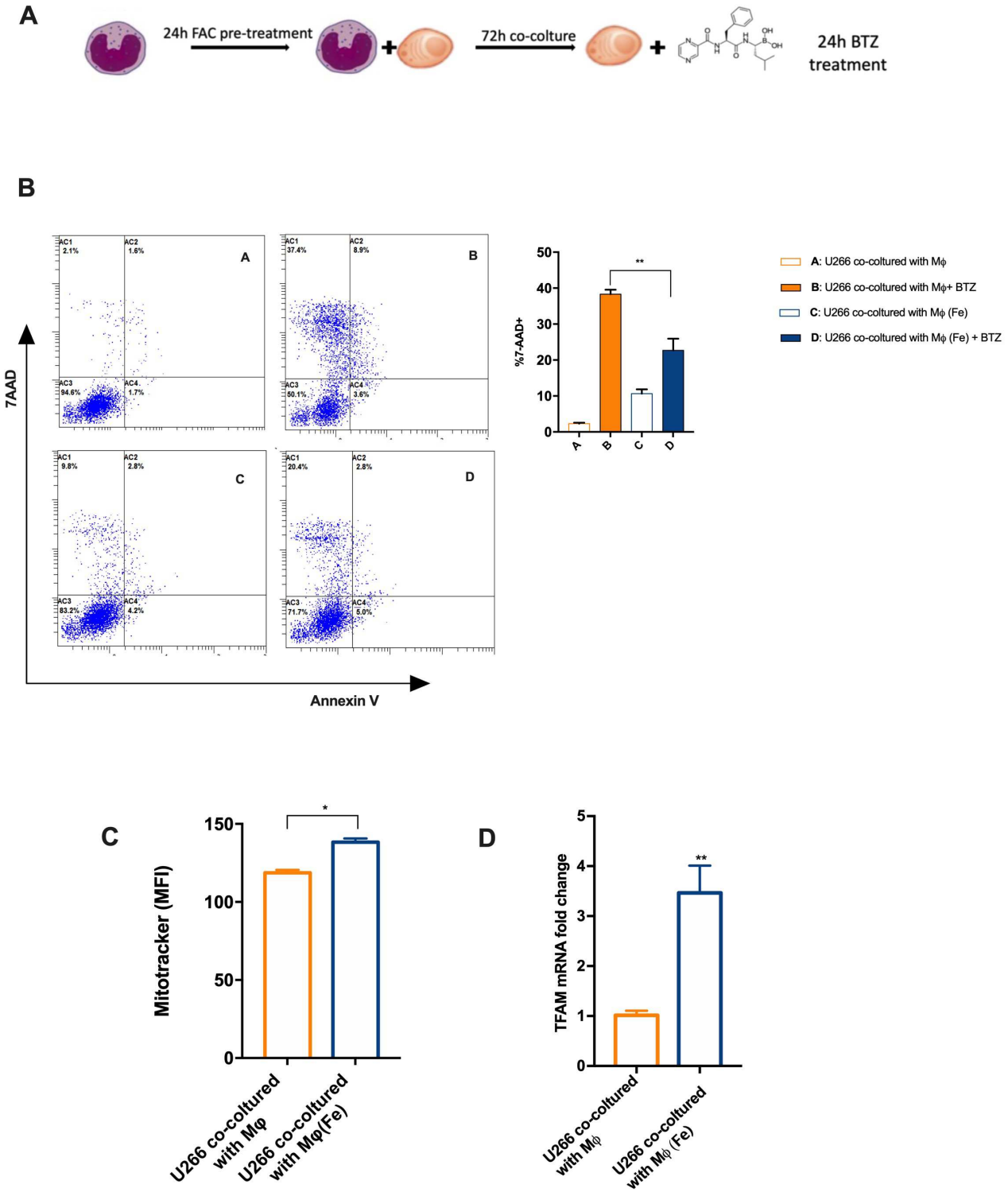
A
24h FAC pre-treatment
72h co-colture
24h BTZ treatment
B
7AAD
Annexin V
A
B
C
D
%7-AAD+
A: U266 co-coltured with Mϕ
B: U266 co-coltured with Mϕ+ BTZ
C: U266 co-coltured with Mϕ (Fe)
D: U266 co-coltured with Mϕ (Fe) + BTZ
C
Mitotracker (MFI)
U266 co-coltured with Mφ
U266 co-coltured with Mφ(Fe)
D
TFAM mRNA fold change
U266 co-coltured with Mϕ
U266 co-coltured with Mϕ (Fe)

Fig. 20: Co-cultured myeloma cells with iron-treated monocytes exert resistance to bortezomib treatment. A. Schematic representation of experiental condition**. B.** U937 cells were pre-treated with FAC 100uM and co-colture with U266 was performed. Apoptosis by FACS analysis of myeloma cells was evaluated after BTZ treatment. A (Co-coltured U266 with untreated U937); B (BTZ treated co-coltured U266 with untreated U937); C (Co-coltured U266 with FAC-treated U937); D (BTZ treated Co-coltured U266 with FAC-treated U937). ***p<0.0001. **C**. Gene expression analysis of mitochondrial biogenesis marker TFAM in co-coltured U266 with U937 cells (alone or after FAC-treatment). Calculated value of 2^-ΔΔCt in untreated U266 cells was 1; **p<0.001. **D.** FACS analysis of mitochondrial mass using MitoTracker Probe. Results are showed as MFI (mean fluorescence intensity. *p<0.01; MΦ (U937).

2.2.3 Zebrafish mpfa4:tomato mutant as model to investigate U266 and U266-Fe xenotranplantation and their interaction with macrophages

Validation of *in vitro* data concerning the role of iron in improvement of myeloma cell proliferation and interaction with macrophages, which play a key role in myeloma microenvironment was performed using zebrafish *mfap4:tomato* mutant. Larvae 2dpf were used to xenotransplantate U266 S and U266-Fe. After 24h and 48h of xenotransplantation in the Cuvier duct of larvae, data proved the presence of myeloma cells (U266S and U266-Fe) in the Caudal Hematopoietic Tissue (CHT) of injected larvae. Interestingly even if FAC 100uM administration to larvae followed by U266 S clone transplantation did not evidence a significant difference compared to the other experimental condition groups [fig. 21A], it was possible to observe a significant interaction (**$p<0.001$) between myeloma cells and macrophages larvae in the CHT after 24h to U266 injection, only when FAC was administrated to larvae [fig. 21B].

Concerning the role of iron in favoring tumor metastasis or tumor cell invasion, it seemed that any significant difference could be observed within the groups [fig. 21C]. Interestingly, even if it was not possible to appreciate a significant increase in tumor metastasis between the groups, it was observed that the percentage of individuals showing metastasis was higher in larvae FAC treated (n=26; 23% at 24h and 26% at 48h) compared to larvae injected with U266 S (n=20; 10% at 24h and 15% at 48h) or U266-Fe (n=26; 15% at both 24 and 48h).

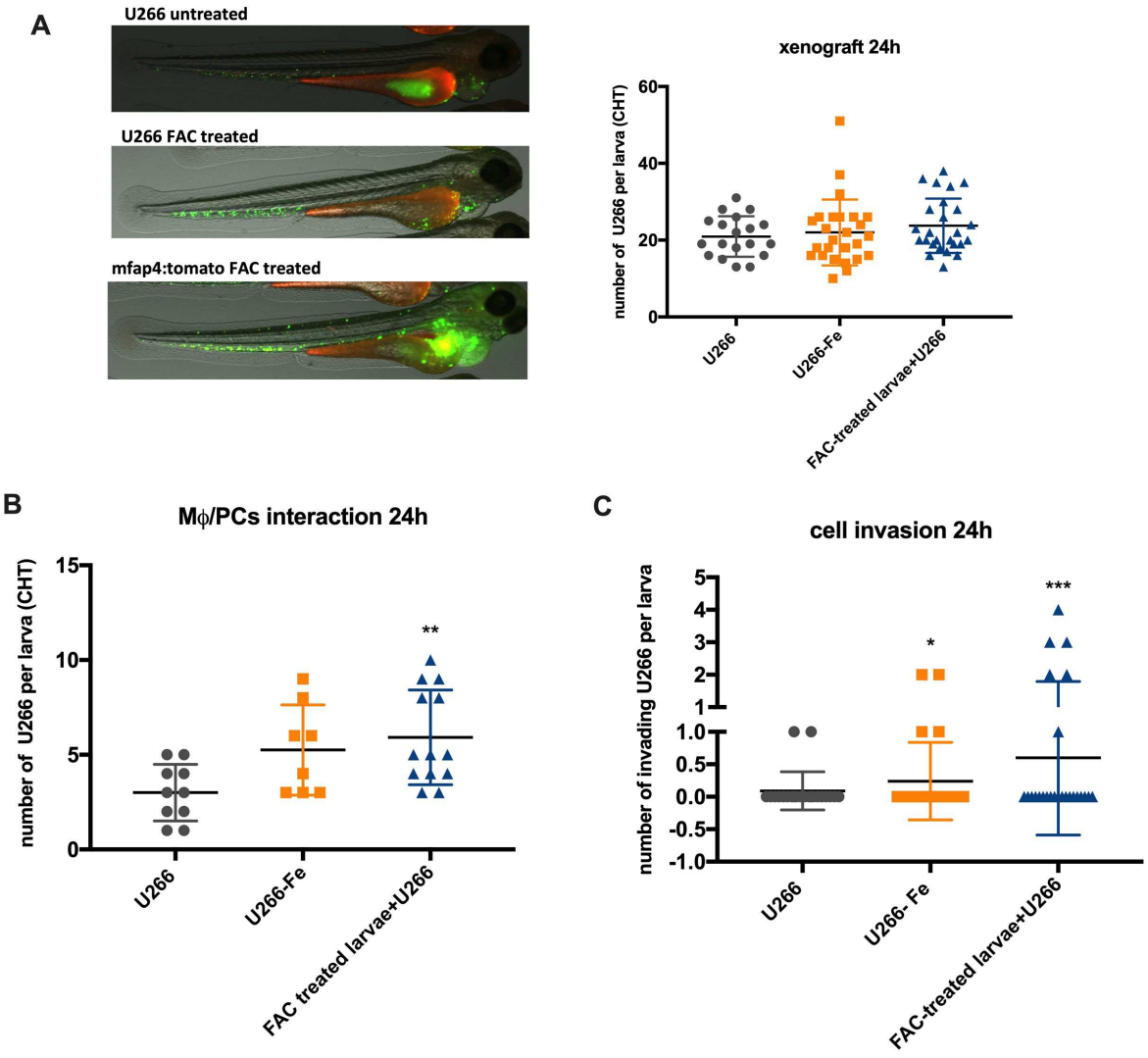

Fig.21: interplay between iron releasing macrophages and myeloma cells *in vivo.* *mfap4:tomato* zebrafish larvae 2dpf xenotranplantated with U266 cells. **A**. Analysis of myeloma cells in the CHT of larvae. **B.** Analysis of MM cells macrophages interaction (yellow puncta) in xenotranplantated larvae. Results are showed as number of myeloma cells in the CHT. **p<0,001. **C.** Analysis of cell invasion was expressed as percentage of individual with metastatic cells in respect with control group (U266 untreated xenotransplantated larvae). U266 untreated (n=20); U266 FAC treated (n=26); *mfap4:tomato* FAC treated (n=26).

2.2.4. Iron loading impairs TNF-a induced M1 polarization *in vivo*

MaiNguyen-Chi et al. identified a polarized macrophages subset in zebrafish using *mpeg1:cherry; tnfa:eGFP* model [Fig. 22A] . To study the inflammatory status of macrophages, TNFa expression in *mpeg1:cherry* cells in fin-wounded larvae was observed. Since iron induced *in vitro* switching from the pro-inflammatory (M1) to the anti-inflammatory (M2) phenotype in macrophages, zebrafish *mpeg1:cherry;tnfa:eGFP* model was used to confirm *in vitro* data. Zebrafish larvae were treated with FAC 100 uM, DFO 100 uM alone and in combination for 24h. Caudal fin amputation was executed on 3dpf larvae and both macrophages recruitment (M2-like; $red^{+}/green^{-}$) and TNFa expressing macrophages(M1-like; $red^{+}/green^{+}$) were observed using a confocal inverted microscope After 6h post inflammation induction. Data highlighted that FAC-treated larvae did not show significant increase of TNFa expression in recruited macrophages of amputated fin compared to untreated larvae (red puncta), while iron chelation induced by DFO treatment was able to increase TNFa expression (**$p<0.005$) in amputed fin macrophages (yellow puncta) compared to FAC-treated and untreated larvae, favoring the pro-inflammatory (M1) phenotype of macrophages [fig. 22B].

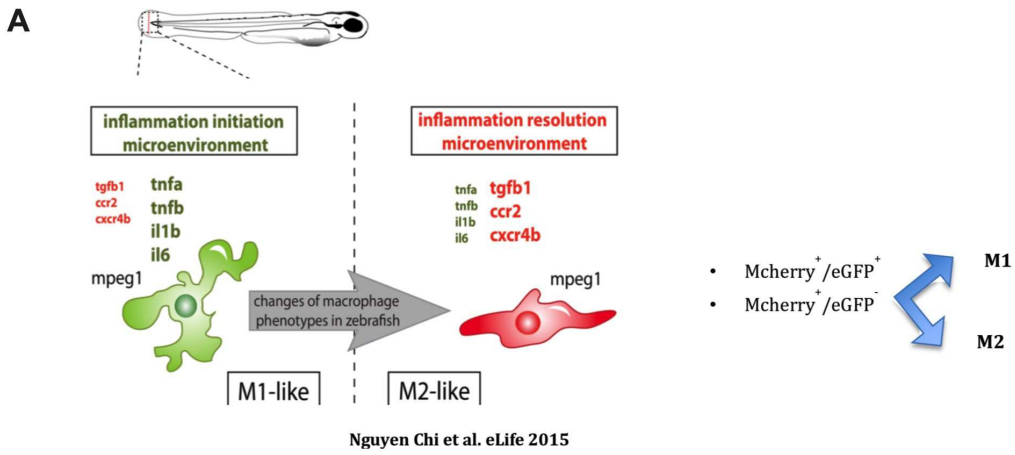

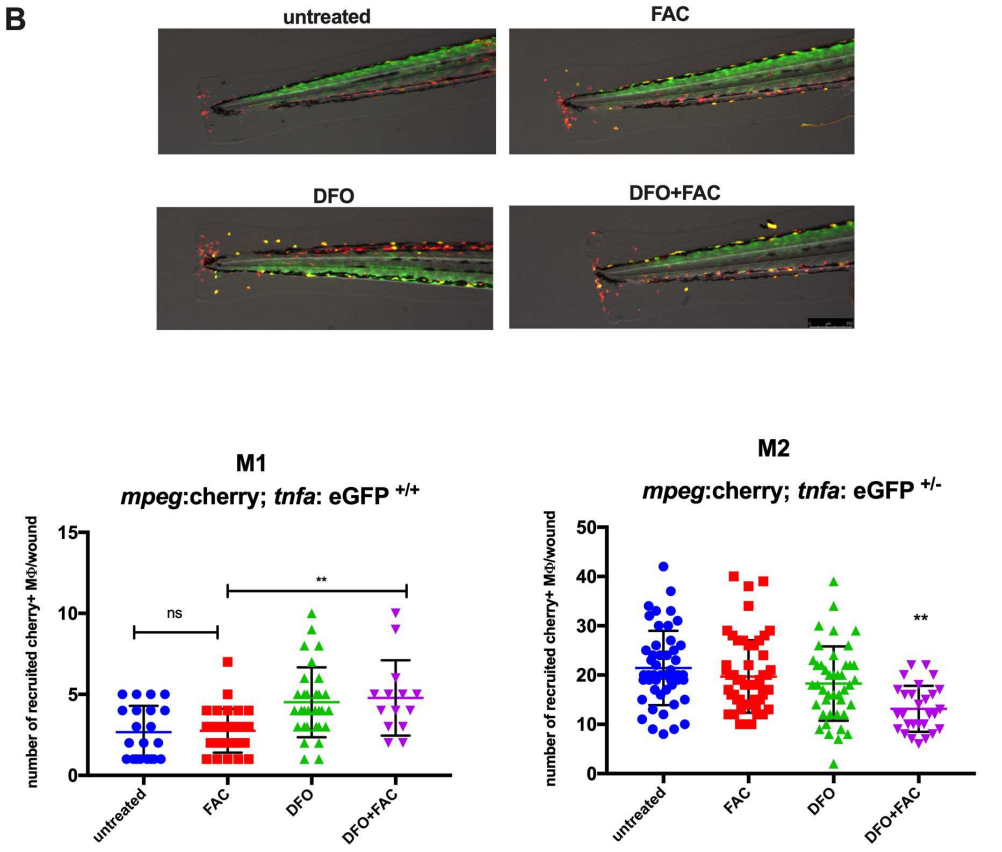

Fig. 22: Iron promotes M2-like phenotype *in vivo*. A. *mpeg1:cherry; TNFa:eGFP* zebrafish model of macrophage polarization. **B**. Dechorionated larvae 1dpf were treated with FAC 100uM alone or in combination with DFO 100uM for 24h. Inflammation stimulus through wounding fin was induced and macrophage recruitment was observed in fin-wound after 6h. M1- like (cherry^{+}; eGFP^{+}: yellow) macrophages and M2-like (cherry^{+};eGFP^{-}: red) were counted in damaged area per larva. **p<0.001. FAC (Ferric Citrate Ammonium); DFO (Deferoxamine).

Discussion

Chapter 1

HDAC6 enzymatic activity inhibition in Multiple Myeloma

Dysregulated HDAC activity is an epigenetic hallmark of cancer, resulting in aberrant gene expression and cellular signaling that promotes cell growth and survival, and resistance to apoptosis [73, 74]. Besides the effect on the acetylation status of histones, HDAC inhibition affects other cellular processes and can lead to a variety of biologic effects downstream important for cellular proliferation, angiogenesis, differentiation and survival. A total of 18 HDACs have been identified and grouped into four classes based on their homology to yeast HDACs, subcellular localization, and enzymatic activities [76]. The classes differ in tissue expression and protein targets [77]. HDAC inhibition has been described as a master switch that could simultaneously affect multiple pathways critical for the survival of MM cells. HDACi inhibit the actions of HDAC enzymes and affect the expression of genes that regulate cancer cell survival via a number of mechanisms. In particular, HDACi bind to the catalytic domains of HDACs, downregulating their activity, which in turn inhibits MM cell survival and proliferation [78]. Concerning the mechanism by which myeloma cells can elude bortezomib efficacy, autophagy is widely thought to contribute to proteasome inhibitor resistance in myeloma by providing an alternative pathway for clearance of dysfunctional proteins. In fact, it is recognised that autophagy can serve two key functions: a tumour-suppressive function through elimination of oncogenic proteins, and perhaps for established cancer, a tumour-promoting function via recycling of metabolites to maintain mitochondrial functionality [37]. Lastly, histone deacetylase 6 (HDAC6) inhibitors and pan-HDAC inhibitors have been evaluated as autophagy inhibitors. HDAC6 is involved in ubiquitin-dependent or ubiquitin-independent protein aggregate formation, as well as their clearance via autophagy [11]. HDAC6, in association with the dynein motor complex, recruits and transports misfolded polyubiquitinated proteins via the microtubule network to aggresomes/autophagosomes for subsequent degradation by lysosome [12].

HDACs have been recently addressed as epigenetic modifiers in regulating immune-modulatory pathway. However, their roles in regulating the immune-related pathways have not been observed completely [41]. Under this context, it is reported that the pharmacological and genetic inhibition of HDAC6 resulted in modulation of expression of co-stimulatory molecules, especially the tumor-associated antigens and MHC class I. Moreover, it seems that HDAC6 is a crucial regulator in the

STAT3 pathways [42], which can be commonly activated in cancer, like osteosarcoma and other malignancies [43].

Authors reported that HDAC6 plays a role in regulating the co-inhibitory molecule PD-L1. This protein is one of the natural ligands for the PD-1 receptor present on T cells, which suppresses T-cell activation, proliferation, and induces T-cell anergy and apoptosis [43]. PD-L1 is found in cancer cells by many important studies [44], [45], and its overexpression is usually related to the poor prognosis of respective malignancies, including osteosarcoma [46], ovarian [47], gastric [48], and breast cancer [49]. Interestingly, we observed that myeloma resistant cells express higher gene levels of HADA6 than the sensitive clone (U266 S) [fig. 5A]. To understand the role of HDAC6 enzymatic activity in myeloma cell resistance, we treated U266 S and U266R with tubacin (inhibitor of HDAC6) and bortezomib. Contrarily to expected results, HDAC6 enzymatic activity inhibiton did not show synergistic effects with bortezomib. It has been reported that HDAC6 plays a role in recruitment and transport of misfolded polyubiquitinated proteins via the microtubule network to aggresomes/autophagosomes for subsequent degradation by lysosome. Our data revealed that HDAC6 inhibition by tubacin treatment did not increase myeloma cell sensivity to bortezomib, since it did not reduce myeloma cells proliferation when coadiministrated with bortezomib in both sensitive (U266) and resistant (U266R) myeloma cells [fig. 5B]. Even if inhibition of aggresomal pathway by HDAC6 inhibition, together with proteasomal inhibition by BTZ resulted in an accumulation of ubiquitinated proteins followed by synergistic anti-MM activity, in our study is not possible to appreciate and confirm previous data [83]. We evaluated autophagy induction by AVO-test in myeloma cells after tubacin and bortezomib treatment, alone or in combination [fig. 6]. Any difference in autophagy modulation after HDAC6 inhibition has been observed in sensitive and resistant myeloma cells after tubacin treatment alone or in combination with bortezomib. Concering HDAC6 ability to modulate co-stimulatory molecules of immune response, this study allowes it to find an interplay between chemical inhibiton of HDAC6 enzymatic activity and gene expression of some immune modulatory factors. We first observed increased expression levels of immuno-modulatory markers as PD-L1 and IL-10 in U266R cells compared to U266 S at basal conditions [fig. 7A]. Treatment with tubacin was able to downregulate the expression levels of both PD-L1 and IL-10 in U266 S and U266 [fig. 7B], thus suggesting a role of HDAC6 enzymatic activity immuno-modulatory molecules regulation. According to Woan, Lienlaf et al. 2015, also in myeloma cells HDAC6 seems to be involved in immune modulatory factors through activaction of pSTAT3. Our data showed that treatment of myeloma cells (U266S and U266 R) with tubacin reduced significantly the percentage of pSTAT3 [fig. 8A]. These data were confirmed using IL-6 as positive control of pSTAT3 induction. In fact, co-treatment of IL-6

and tubacin showed significantly decrease of pSTAT3 percentage in myeloma cells, compared to IL-6 alone [fig. 8].

In conclusion, this part of the research work highlighted that HDAC6 enzymatic activity inhibition did not seem to be involved in improvement of bortezomib toxicity in myeloma cells, since we did not appreciate a synergistic action between HDAC6 inhibition and bortezomib cytotoxicity. It is possible to speculate a major efficacy of HDAC6 inhibition in modulation of immuno modulatory factors. To this regard, considering the interplay between MM cells and tumor microenvironment in tumor progression, it could be interesting to explore the properties of HDAC6 in microenvironment cell components such as macrophages, mesenchymal stromal cells, T-cells, neutrophils, focusing attention on deregulated pathways involved in immusuppressive functions exerted by cells in tumor microenviroment.

Chapter 2

Iron as key player on inducing myeloma cell resistance through promoting macrophage polarization in tumor microenvironment

The malignant cancer phenotype is often found in association with a deregulated iron homeostasis, particularly the expression of iron-regulated genes that fuel their higher metabolic iron demands needed for division, growth, and survival [25]. This surplus of iron is needed not only both during early steps of tumor development, e.g., enhanced survival [26] and proliferation of transformed cells [27], but also during late stages to promote the metastatic cascade. Also, iron is crucial in remodeling the extracellular matrix and increasing the motility and invasion of cancer cells [8]. Interengly, we found that U266 R cells showed higher gene expression levels of FPN, DMT1 and TFRC1 than U266 S at basal conditions [fig. 9] Apparently, the expression of different iron-regulated genes such as the transferrin receptor (TfR1), ferritin light chain (FTL) [55], and the iron regulatory protein (IRP)-2 [40] in tumor cells correlated with a poor prognosis, a higher tumor grade, and increased chemoresistance. It is well known that increased iron trafficking gene levels as FPN or TFRC1 are linked to deregulated iron metabolism in cancer cells. Tumor cells adjust intracellular iron metabolism to favour iron accumulation, by increasing iron uptake and storage, at the same time decreasing iron export [4]; [54]. Imported iron enters the bioactive labile iron pool (LIP), which provides it for metabolic and proliferative purposes. The amount of the LIP is sensed by post-transcriptional mechanisms of cytosolic iron-regulated RNA binding proteins 1 and 2 (IRP-1 and IRP-2) to uptake, storage, and release of iron Gnaiger et al. 1999, Netz, Stith et al. 2011). Also, the ability of iron to get oxidized or reduced enables iron to take part in free radical

generating reactions. Among them is the Fenton reaction in which ferrous iron donates an electron to hydrogen peroxide to produce the hydroxyl radical, a highly reactive oxygen species.

As a result, iron is potentially mutagenic by causing DNA strand breaks, which provokes cellular transformations, or induces protein as well as lipid modifications within malignant cells, causing a more aggressive tumor cell behavior [15], [50]. Exploring the mechanisms of bortezomib resistance in myeloma cells, in this study it has been found that iron allow to myeloma cells to acquire resistance to bortezomib treatment. In sensitive myeloma cells bortezomib reduce cell viability, exerting its toxic properties. Authors reported that Bortezomib treatment induce myeloma cells damage through induction of proteotoxic stress and increasing oxidative stress levels [93]. As far as concerns the mechanisms of pharmacological resistance altered redox balance of cancer cells have been proposed as a possible mechanism of chemoresistance. To this regard, cancer cells exhibit persistent reactive oxygen (ROS) species levels leading to an adaptive stress responses and allowing cancer cells to survive with elevated levels of ROS and preserve cellular viability [28]. In neoplasia, cancer cells often have altered cell-death pathways and mitochondrial functions that allow them to escape cell-death programs [94]. Authors, also, have shown in MM cells that mitochondrial activity is a determining factor in the regulation of apoptosis resistance in response to bortezomib, since ROS accumulation induced increased mitochondrial gene expression serve as a source of drug resistance under apoptotic or stressed conditions [95]. Here we showed that iron treatmet modify the energetic metabolism status of myeloma cells allow them to elude the effects of drug treatment. We treated myeloma cell lines with iron and proved the ability of myeloma cells to internalize iron. Gene expression analysis revealed significant increased levels of iron trafficking genes as FPN and TFRC1 and also increasing LIP content when cells were treated with iron [fig.10A, B]. Since iron treatment did not affect myeloma cell viability [fig.10 C], we decided to investigate the mechanisms by which iron could modify MM cells response to bortezomib. We first observed increasing oxidative stress through ROS production and significant upregulation of oxidative stress genes as SOD2, HMOX-1, GLUT-S-TRANSF and CYTB [fig. 11 A, B]. Also, mitochondrial membrane depolarization damage was recovered after 24h and was accomplished by increased mitochondrial mass and increased levels of mitochondrial biogenesis markers as TFAM and ND4 [fig.12], thus confirming improved mitochondria functions. We found that iron treatment resulted in acquisition of MM cells resitance to bortezomib treatment. We pre-treated U266 cells with iron (U266-Fe), we next added bortezomib and evualated U266-Fe response to bortezomib treatment compared to U266 S. Our data highlighted that iron pre-treatment in myeloma cells

decreases apoptotic rate after bortezomib addiction compared to U266 S [fig. 14A]. To prove the ability of iron in reducing myeloma cells sensivity to bortezomib, we next treated U266-Fe with the iron chelator Deferasixor (DFX) and the added bortezomib. Results showed that myeloma cells abolished their resistance to bortezomib when iron was chelated by DFX [fig. 15B].

Investigation of mechamisms by which iron could modify bortezomib response in MM cells, allow us to find that while in U266 S cells bortezomib treatment damages mitochondrial functions, iron treatment allow them to protect to damage induced by bortezomib administration, through improvement of mitochondrial function, according to [95]. We observed that U266-Fe treated with iron did not icrease ROS production and they did not downregulate gene expression of mitochondria fitness markers as ND4 and CYTB, whereas U266 S responded to bortezomib induced damage increasing ROS and reducing expression levels of NDA4 and CYTB [fig. 16 A, B]. The hypothesis that iron could be involved in bortezomib resistance in myeloma model was also evaluated *in vivo*. Developing a zebrafish model for assessment of tumor cell homing and metastasis to the BM by injecting either MM cell lines or patient-derived MM cells into zebrafish embryos and demonstrating their homing to the caudal hematopoietic tissue (CHT) where the HSCs migrate after their emergence from the ventral wall of the dorsal aorta gained great interest in the last years. Sacco et al. first demonstrated the homing ability of MM cells in CHT of zebrafish embryos, while [96] assessed the possibility to use zebrafish as model to evaluate not only the engraftment of MM cell line and primary $CD138^{+}$ cells, but also the efficacy of several drugs against MM cells. Since zebrafish could be considered a representative tool to study myeloma biology, we explored ability of iron to induce bortezomib resistance using zebrafish casper larve xenotransplanted U266 S and U266-Fe. We treated xenotranplated larvae with bortezomib up to 48h and then evaluated the presence of myeloma cells in CHT. Our data showed that bortezomib treatment reduced U266 S cell number, whereas it was not possible to observe a reduction of U266-Fe cells after bortezomib treatment in the CHT [Fig. 16 A, B]. Since bortezomib treatment of xenotransplantated larvae with U266-Fe cells did non show its efficacy in reducing the number of cells in the CHT, our data provide the key player role of iron in inducing bortezomib resistance also in *in vivo* model.

The role of iron for cancer development is tightly linked to its ability to modulate innate adaptive immune responses of macrophages or T cells. During early stages of carcinogenesis, pro-inflammatory cytokines endorse iron sequestration in macrophages and enhance the production of reactive oxygen species as a firstline anti-tumor defense. Chronic inflammation or smoldering, inflammation often creates an equilibrium between killing of immunogenic tumor cells and immune finally driving tumor outgrowth. Outgrowth is supported as tumor cells often evade recognition or even acquire an immunosuppressive phenotype [56]. The appearance of tumor-supporting, iron-donating immune cells, in particular macrophages, is associated with tumor size and aggressiveness as well as poor patient prognosis [58]; [59]. Anti-inflammatory macrophages are predisposed to iron export and the distribution of iron to the extracellular space, whereas iron storage is reduced. As alternatively activated macrophages scavenge senescent and/or apoptotic cells [63], they play an important role in tissue repair, regeneration, resolution of inflammation, and iron recycling. While pro-inflammatory macrophages (M1) are prone to iron retention, display an iron sequestering phenotype characterized by enhanced iron uptake and storage but attenuated its release [62], while anti-inflammatory macrophages (M2) are predisposed to iron export and the distribution of iron to the extracellular space, whereas iron storage is reduced. Also, it has been provided that TAMs (M2) adopt an iron-release phenotype due to their interaction with dying tumor cells, whereby iron availability was increased within the tumor microenvironment. Under these conditions, TAMs expressed higher levels of the high-affinity iron-binding protein lipocalin-2 (Lcn-2). Lcn-2 turned out to export iron from TAM, allowing to cancer cells to acquire iron in the tumor microevironment [64]. Iron metabolism is significantly altered in multiple myeloma (MM). Availability of iron for the developing erythrocytes becomes limiting resulting in the characteristic anemia so frequently seen in this disease. There are several potential etiologies for myeloma-associated anemia that have been considered. Certainly, the extensive BM involvement with malignant cells can theoretically result in decreased capacity for functional erythropoiesis [67]. Also, it has been reported that malignant plasma cells have increased expression of Fas ligand on their surface which may cause apoptosis of erythroid precursors within the marrow [57], although the mechanisms by which iron in tumor microenvironment guide macrophage polarization and tumor progression have to be elucidated. In the present work, we explored the role of iron on promoting macrophages polarization switch. We first treated U937 monocyte cell line with iron and proved that they internalize iron, since we observed increased expression levels of iron trafficking genes as FPN and DMT1, accomplished with increased gene expression of the main scavenger gene HMOX-1 [Fig. 17A].

Our data also demonstrated that iron impairs macrophage polarization towards M2 phenotype, since we founded increased levels of CD206 and significant reduction of HLA-DR [fig. 18 A]. Authors [97] reported the role of Arginase 1 (ARG1) enzymatic activity in immunosuppression of DC cells, accomplished to expression of TGFb cytokine expression. Our data showed that iron induced ARG1 and TGFb expression in macrophages [fig. 18 B], thus providing the ability to promote M2 phenotype *in vitro*. Also, treatment of human primary monocytes with iron confirmed the switch of macrophages phenotype towards M2 like. We observe increase levels of CD206 and decreased HLA-DR by FACS in iron treated human monocytes. We next explored the role of iron in guiding macrophages polatization using zebrafish model. *mpeg1:chrry; tnfa:eGFP* zebrafish [98] was used to track the switch of phenotype of macrophages, inducing inflammatory stimulus through fin wounded. We treated zebrafish larvae with iron, alone or in combination with iron chelator Deferoxamine (DFO) for 24h. To evaluate macrophages polarization, we performed fin wound and observed macrophages recruitment [fig. 22A]. Accoding to recently published data [99], our data showed that increased cell iron loading triggers the expression of monocyte polarization markers of M2-like phenotype in recruited macrophages and dampens pro-inflammatory immune responses, while iron deficiency has the opposite effect. In fact, we observed increased expression of TNFa in macrophages treated with deferoxamine, whereas macrophages of iron treated larvse did non show significant increase of TNFa expression [fig. 22 B]. Our *in vivo* data suggest that increased iron status did not lead to increasing expression of pro-inflammatory markers as TNFa, linked to M1-like phenotype.

These data suggest the involvement of iron in resolution of inflammatory stimulus, supporting the idea that in tumor microenvironment iron realesed by macrophages could promote anti-inflammatory and immunosuppressive activation mechanisms. Therefore, changes in cell iron concentration can modulate macrophage phenotype and function with clear implications for the immune responses. Concerning the link existing between the property of M2 macrophages to release iron and the role of iron in favoring MM cells bortezomib resistance, we pre- treated U937 cells. We next performed a co-colture with U266 cells that were then treated with bortezomib for 24h [fig. 21A]. Our data showed that co-cultured U266 S with U937 treated with iron acquire resistance to bortezomib treatment, probably through iron mobilization from U937 to U266 cells. We observed that co-cultured U266 S with U937 treated with iron reduced their sensitivity to bortezomib treatment compared to U266 S co-coltured with untreated U937 cells by apoptosis evaluation [fig. 20 B].

Since we found increased expression levels of TFAM (as mitochondrial biogenesis marker) in U266 co-cultured with U937 pre-treated with iron, accomplished with increased mitochondrial mass [fig. 20 C], we hyphotized that the interplay between macrophages (MΦ) and MM cells promote bortezomib resistance through iron trafficking. We next explored the interplay between macrophages iron-loaded and MM cells *in vivo,* using *mfap4: tomato* zebrafish larvae. Our data highlighted a significant MΦ/MM cells interaction in the CHT when larvae were pre-treated with iron [Fig.22 A], suggesting a role of macrophages iron-loaded in releasing iron in tumor microenvironment. Moreover, our data allow us to observe that iron- pretreated larvae with iron were able to promote U266 cell invasion out of the CHT, compared to untreated larvae [Fig. 21 B]. Our results proved a key role of iron-loaded macrophages to promote tumor progression, even if the mechanisms by which macrophages exert their interaction with MM cells have to be elucidated.

These data highlight the interplay between macrophages iron-loaded cells, bortezomib resistance of myeloma cells and tumor microenvironment. Indeed, iron trafficking, through modifying energetic metabolism of cancer cells and imparing inflammatory status of macrophages, is able to promote mechanisms of bortezomib resistance in myeloma cells and also macrophages polarization toward immunosuppressive phenotype (M2), *in vitro* and *in vivo* models. In conclusion, targeting iron trafficking in myeloma cells could be a promising strategy to revert bortezomib resistance, even if a better understanding of iron metabolism in tumor microenvironment cells, as macrophages, is needed, considering the multifactorial component of the microenvironment that alter several processes and pathways contributing to the progression disease.

References

1. Siegel, R.L., K.D. Miller, and A. Jemal, *Cancer statistics, 2016.* CA Cancer J Clin, 2016. **66**(1): p. 7-30.
2. Drayson, M., et al., *Serum free light-chain measurements for identifying and monitoring patients with nonsecretory multiple myeloma.* Blood, 2001. **97**(9): p. 2900-2.
3. Turesson, I., et al., *Patterns of multiple myeloma during the past 5 decades: stable incidence rates for all age groups in the population but rapidly changing age distribution in the clinic.* Mayo Clin Proc, 2010. **85**(3): p. 225-30.
4. Kyle, R.A., et al., *Review of 1027 patients with newly diagnosed multiple myeloma.* Mayo Clin Proc, 2003. **78**(1): p. 21-33.
5. Rajkumar, S.V., et al., *International Myeloma Working Group updated criteria for the diagnosis of multiple myeloma.* Lancet Oncol, 2014. **15**(12): p. e538-48.
6. Kyle, R.A., et al., *Clinical course and prognosis of smoldering (asymptomatic) multiple myeloma.* N Engl J Med, 2007. **356**(25): p. 2582-90.
7. Boone, B.A., et al., *Safety and Biologic Response of Pre-operative Autophagy Inhibition in Combination with Gemcitabine in Patients with Pancreatic Adenocarcinoma.* Ann Surg Oncol, 2015. **22**(13): p. 4402-10.
8. Wu, Y., et al., *Synthesis and screening of 3-MA derivatives for autophagy inhibitors.* Autophagy, 2013. **9**(4): p. 595-603.
9. Yao, T.P., *The role of ubiquitin in autophagy-dependent protein aggregate processing.* Genes Cancer, 2010. **1**(7): p. 779-786.
10. Kawaguchi, Y., et al., *The deacetylase HDAC6 regulates aggresome formation and cell viability in response to misfolded protein stress.* Cell, 2003. **115**(6): p. 727-38.
11. Iwata, A., et al., *HDAC6 and microtubules are required for autophagic degradation of aggregated huntingtin.* J Biol Chem, 2005. **280**(48): p. 40282-92.
12. Ouyang, H., et al., *Protein aggregates are recruited to aggresome by histone deacetylase 6 via unanchored ubiquitin C termini.* J Biol Chem, 2012. **287**(4): p. 2317-27.
13. Dimopoulos, M., et al., *Vorinostat or placebo in combination with bortezomib in patients with multiple myeloma (VANTAGE 088): a multicentre, randomised, double-blind study.* Lancet Oncol, 2013. **14**(11): p. 1129-1140.
14. Yagi, T., et al., *Tumour-associated macrophages are associated with poor prognosis and programmed death ligand 1 expression in oesophageal cancer.* Eur J Cancer, 2019. **111**: p. 38-49.
15. Inoue, S. and S. Kawanishi, *Hydroxyl radical production and human DNA damage induced by ferric nitrilotriacetate and hydrogen peroxide.* Cancer Res, 1987. **47**(24 Pt 1): p. 6522-7.
16. Roodman, G.D., *Mechanisms of bone lesions in multiple myeloma and lymphoma.* Cancer, 1997. **80**(8 Suppl): p. 1557-63.
17. Roodman, G.D., *Pathogenesis of myeloma bone disease.* Leukemia, 2009. **23**(3): p. 435-41.
18. Coyte, P.C., *Current trends in Canadian health care: myths and misconceptions in health economics.* J Public Health Policy, 1990. **11**(2): p. 169-88.
19. Hofman, I.J.F., et al., *Low frequency mutations in ribosomal proteins RPL10 and RPL5 in multiple myeloma.* Haematologica, 2017. **102**(8): p. e317-e320.
20. Chauhan, D., et al., *Blockade of Hsp27 overcomes Bortezomib/proteasome inhibitor PS-341 resistance in lymphoma cells.* Cancer Res, 2003. **63**(19): p. 6174-7.
21. Guerrero-Garcia, T.A., et al., *The power of proteasome inhibition in multiple myeloma.* Expert Rev Proteomics, 2018. **15**(12): p. 1033-1052.

22. Ruckrich, T., et al., *Characterization of the ubiquitin-proteasome system in bortezomib-adapted cells.* Leukemia, 2009. **23**(6): p. 1098-105.
23. Hofman, I.J.F., et al., *RPL5 on 1p22.1 is recurrently deleted in multiple myeloma and its expression is linked to bortezomib response.* Leukemia, 2017. **31**(8): p. 1706-1714.
24. Raedler, L., *Velcade (Bortezomib) Receives 2 New FDA Indications: For Retreatment of Patients with Multiple Myeloma and for First-Line Treatment of Patients with Mantle-Cell Lymphoma.* Am Health Drug Benefits, 2015. **8**(Spec Feature): p. 135-40.
25. Masella, R., et al., *Protocatechuic acid and human disease prevention: biological activities and molecular mechanisms.* Curr Med Chem, 2012. **19**(18): p. 2901-17.
26. Meister, S., et al., *Extensive immunoglobulin production sensitizes myeloma cells for proteasome inhibition.* Cancer Res, 2007. **67**(4): p. 1783-92.
27. Nakamura, M., et al., *Activation of the endoplasmic reticulum stress pathway is associated with survival of myeloma cells.* Leuk Lymphoma, 2006. **47**(3): p. 531-9.
28. Zhang, L., J.H. Fok, and F.E. Davies, *Heat shock proteins in multiple myeloma.* Oncotarget, 2014. **5**(5): p. 1132-48.
29. Tibullo, D., et al., *Nuclear translocation of heme oxygenase-1 confers resistance to imatinib in chronic myeloid leukemia cells.* Curr Pharm Des, 2013. **19**(15): p. 2765-70.
30. Kushida, T., et al., *TNF-alpha-mediated cell death is attenuated by retrovirus delivery of human heme oxygenase-1 gene into human microvessel endothelial cells.* Transplant Proc, 2002. **34**(7): p. 2973-8.
31. Vander Heiden, M.G., L.C. Cantley, and C.B. Thompson, *Understanding the Warburg effect: the metabolic requirements of cell proliferation.* Science, 2009. **324**(5930): p. 1029-33.
32. Peppicelli, S., et al., *The acidic microenvironment as a possible niche of dormant tumor cells.* Cell Mol Life Sci, 2017. **74**(15): p. 2761-2771.
33. Koukourakis, M.I., et al., *Metabolic cooperation between co-cultured lung cancer cells and lung fibroblasts.* Lab Invest, 2017. **97**(11): p. 1321-1331.
34. Webb, B.A., et al., *Dysregulated pH: a perfect storm for cancer progression.* Nat Rev Cancer, 2011. **11**(9): p. 671-7.
35. Peppicelli, S., et al., *Metformin is also effective on lactic acidosis-exposed melanoma cells switched to oxidative phosphorylation.* Cell Cycle, 2016. **15**(14): p. 1908-18.
36. Zheng, J., *Energy metabolism of cancer: Glycolysis versus oxidative phosphorylation (Review).* Oncol Lett, 2012. **4**(6): p. 1151-1157.
37. White, E., *Deconvoluting the context-dependent role for autophagy in cancer.* Nat Rev Cancer, 2012. **12**(6): p. 401-10.
38. Lambert, L.A., et al., *Autophagy: a novel mechanism of synergistic cytotoxicity between doxorubicin and roscovitine in a sarcoma model.* Cancer Res, 2008. **68**(19): p. 7966-74.
39. Verfaillie, T., et al., *Linking ER Stress to Autophagy: Potential Implications for Cancer Therapy.* Int J Cell Biol, 2010. **2010**: p. 930509.
40. Poklepovic, A. and D.A. Gewirtz, *Outcome of early clinical trials of the combination of hydroxychloroquine with chemotherapy in cancer.* Autophagy, 2014. **10**(8): p. 1478-80.
41. Perham, R.N., et al., *Substrate channelling in 2-oxo acid dehydrogenase multienzyme complexes.* Biochem Soc Trans, 2002. **30**(2): p. 47-51.
42. Woan, K.V., et al., *Targeting histone deacetylase 6 mediates a dual anti-melanoma effect: Enhanced antitumor immunity and impaired cell proliferation.* Mol Oncol, 2015. **9**(7): p. 1447-1457.
43. Tu, B., et al., *STAT3 activation by IL-6 from mesenchymal stem cells promotes the proliferation and metastasis of osteosarcoma.* Cancer Lett, 2012. **325**(1): p. 80-8.
44. Tomasi, T.B., W.J. Magner, and A.N. Khan, *Epigenetic regulation of immune escape genes in cancer.* Cancer Immunol Immunother, 2006. **55**(10): p. 1159-84.

45. Pardoll, D.M., *The blockade of immune checkpoints in cancer immunotherapy.* Nat Rev Cancer, 2012. **12**(4): p. 252-64.
46. Lussier, D.M., et al., *Combination immunotherapy with alpha-CTLA-4 and alpha-PD-L1 antibody blockade prevents immune escape and leads to complete control of metastatic osteosarcoma.* J Immunother Cancer, 2015. **3**: p. 21.
47. Darb-Esfahani, S., et al., *Prognostic impact of programmed cell death-1 (PD-1) and PD-ligand 1 (PD-L1) expression in cancer cells and tumor-infiltrating lymphocytes in ovarian high grade serous carcinoma.* Oncotarget, 2016. **7**(2): p. 1486-99.
48. Boger, C., et al., *PD-L1 is an independent prognostic predictor in gastric cancer of Western patients.* Oncotarget, 2016. **7**(17): p. 24269-83.
49. Chen, S., et al., *PD-L1 expression of the residual tumor serves as a prognostic marker in local advanced breast cancer after neoadjuvant chemotherapy.* Int J Cancer, 2017. **140**(6): p. 1384-1395.
50. Thanan, R., et al., *Inflammation-induced protein carbonylation contributes to poor prognosis for cholangiocarcinoma.* Free Radic Biol Med, 2012. **52**(8): p. 1465-72.
51. Lu, B., et al., *The Role of Ferroptosis in Cancer Development and Treatment Response.* Front Pharmacol, 2017. **8**: p. 992.
52. Netz, D.J., et al., *Eukaryotic DNA polymerases require an iron-sulfur cluster for the formation of active complexes.* Nat Chem Biol, 2011. **8**(1): p. 125-32.
53. Oexle, H., E. Gnaiger, and G. Weiss, *Iron-dependent changes in cellular energy metabolism: influence on citric acid cycle and oxidative phosphorylation.* Biochim Biophys Acta, 1999. **1413**(3): p. 99-107.
54. Volani, C., et al., *Dietary iron loading negatively affects liver mitochondrial function.* Metallomics, 2017. **9**(11): p. 1634-1644.
55. Sui, X., et al., *Autophagy and chemotherapy resistance: a promising therapeutic target for cancer treatment.* Cell Death Dis, 2013. **4**: p. e838.
56. Lee, P., et al., *Regulation of hepcidin transcription by interleukin-1 and interleukin-6.* Proc Natl Acad Sci U S A, 2005. **102**(6): p. 1906-10.
57. Silvestris, F., et al., *Negative regulation of erythroblast maturation by Fas-L(+)/TRAIL(+) highly malignant plasma cells: a major pathogenetic mechanism of anemia in multiple myeloma.* Blood, 2002. **99**(4): p. 1305-13.
58. Daniels, T.R., et al., *The transferrin receptor part I: Biology and targeting with cytotoxic antibodies for the treatment of cancer.* Clin Immunol, 2006. **121**(2): p. 144-58.
59. Kalinowski, D.S. and D.R. Richardson, *The evolution of iron chelators for the treatment of iron overload disease and cancer.* Pharmacol Rev, 2005. **57**(4): p. 547-83.
60. Chitambar, C.R., *Medical applications and toxicities of gallium compounds.* Int J Environ Res Public Health, 2010. **7**(5): p. 2337-61.
61. Harris, W.R. and V.L. Pecoraro, *Thermodynamic binding constants for gallium transferrin.* Biochemistry, 1983. **22**(2): p. 292-9.
62. Kisselev, A.F. and A.L. Goldberg, *Proteasome inhibitors: from research tools to drug candidates.* Chem Biol, 2001. **8**(8): p. 739-58.
63. Ng, P.P., et al., *Molecular events contributing to cell death in malignant human hematopoietic cells elicited by an IgG3-avidin fusion protein targeting the transferrin receptor.* Blood, 2006. **108**(8): p. 2745-54.
64. Gozzelino, R. and M.P. Soares, *Coupling heme and iron metabolism via ferritin H chain.* Antioxid Redox Signal, 2014. **20**(11): p. 1754-69.
65. Cairo, G., et al., *Iron trafficking and metabolism in macrophages: contribution to the polarized phenotype.* Trends Immunol, 2011. **32**(6): p. 241-7.
66. Soares, M.P. and I. Hamza, *Macrophages and Iron Metabolism.* Immunity, 2016. **44**(3): p. 492-504.

67. VanderWall, K., et al., *Iron in multiple myeloma.* Crit Rev Oncog, 2013. **18**(5): p. 449-61.
68. Mittelman, M., *The implications of anemia in multiple myeloma.* Clin Lymphoma, 2003. **4 Suppl 1**: p. S23-9.
69. Cremieux, P.Y., et al., *Cost of outpatient blood transfusion in cancer patients.* J Clin Oncol, 2000. **18**(14): p. 2755-61.
70. Rivera, S., et al., *Hepcidin excess induces the sequestration of iron and exacerbates tumor-associated anemia.* Blood, 2005. **105**(4): p. 1797-802.
71. Nemeth, E., et al., *Hepcidin regulates cellular iron efflux by binding to ferroportin and inducing its internalization.* Science, 2004. **306**(5704): p. 2090-3.
72. Rodriguez, J.A., et al., *Lethal iron deprivation induced by non-neutralizing antibodies targeting transferrin receptor 1 in malignant B cells.* Leuk Lymphoma, 2011. **52**(11): p. 2169-78.
73. West, A.C. and R.W. Johnstone, *New and emerging HDAC inhibitors for cancer treatment.* J Clin Invest, 2014. **124**(1): p. 30-9.
74. Stimson, L., et al., *HDAC inhibitor-based therapies and haematological malignancy.* Ann Oncol, 2009. **20**(8): p. 1293-302.
75. Naymagon, L. and M. Abdul-Hay, *Novel agents in the treatment of multiple myeloma: a review about the future.* J Hematol Oncol, 2016. **9**(1): p. 52.
76. Gregoretti, I.V., Y.M. Lee, and H.V. Goodson, *Molecular evolution of the histone deacetylase family: functional implications of phylogenetic analysis.* J Mol Biol, 2004. **338**(1): p. 17-31.
77. Cea, M., et al., *New insights into the treatment of multiple myeloma with histone deacetylase inhibitors.* Curr Pharm Des, 2013. **19**(4): p. 734-44.
78. Libby, E.N., et al., *Panobinostat: a review of trial results and future prospects in multiple myeloma.* Expert Rev Hematol, 2015. **8**(1): p. 9-18.
79. Xu, W., et al., *Intrinsic apoptotic and thioredoxin pathways in human prostate cancer cell response to histone deacetylase inhibitor.* Proc Natl Acad Sci U S A, 2006. **103**(42): p. 15540-5.
80. Miki, Y., et al., *Accumulation of histone deacetylase 6, an aggresome-related protein, is specific to Lewy bodies and glial cytoplasmic inclusions.* Neuropathology, 2011. **31**(6): p. 561-8.
81. Rosato, R.R., J.A. Almenara, and S. Grant, *The histone deacetylase inhibitor MS-275 promotes differentiation or apoptosis in human leukemia cells through a process regulated by generation of reactive oxygen species and induction of p21CIP1/WAF1 1.* Cancer Res, 2003. **63**(13): p. 3637-45.
82. Glozak, M.A. and E. Seto, *Histone deacetylases and cancer.* Oncogene, 2007. **26**(37): p. 5420-32.
83. Hideshima, T., P.G. Richardson, and K.C. Anderson, *Mechanism of action of proteasome inhibitors and deacetylase inhibitors and the biological basis of synergy in multiple myeloma.* Mol Cancer Ther, 2011. **10**(11): p. 2034-42.
84. Kikuchi, J., et al., *Histone deacetylases are critical targets of bortezomib-induced cytotoxicity in multiple myeloma.* Blood, 2010. **116**(3): p. 406-17.
85. Chen, S., et al., *A Bim-targeting strategy overcomes adaptive bortezomib resistance in myeloma through a novel link between autophagy and apoptosis.* Blood, 2014. **124**(17): p. 2687-97.
86. Arunachalam, M., et al., *Natural history of zebrafish (Danio rerio) in India.* Zebrafish, 2013. **10**(1): p. 1-14.
87. Lawrence, C., *Advances in zebrafish husbandry and management.* Methods Cell Biol, 2011. **104**: p. 429-51.

88. Baudino, T.A., et al., *c-Myc is essential for vasculogenesis and angiogenesis during development and tumor progression.* Genes Dev, 2002. **16**(19): p. 2530-43.
89. Mezquita, P., et al., *Myc regulates VEGF production in B cells by stimulating initiation of VEGF mRNA translation.* Oncogene, 2005. **24**(5): p. 889-901.
90. Roccaro, A.M., et al., *SDF-1 inhibition targets the bone marrow niche for cancer therapy.* Cell Rep, 2014. **9**(1): p. 118-128.
91. Sacco, A., et al., *Cancer Cell Dissemination and Homing to the Bone Marrow in a Zebrafish Model.* Cancer Res, 2016. **76**(2): p. 463-71.
92. Keremu, A., et al., *Role of the HDAC6/STAT3 pathway in regulating PD-L1 expression in osteosarcoma cell lines.* Cancer Chemother Pharmacol, 2019. **83**(2): p. 255-264.
93. Tibullo, D., et al., *Heme oxygenase-1 nuclear translocation regulates bortezomibinduced cytotoxicity and mediates genomic instability in myeloma cells.* Oncotarget, 2016. **7**(20): p. 28868-80.
94. Gogvadze, V., S. Orrenius, and B. Zhivotovsky, *Mitochondria in cancer cells: what is so special about them?* Trends Cell Biol, 2008. **18**(4): p. 165-73.
95. Song, I.S., et al., *Mitochondrial modulation decreases the bortezomib-resistance in multiple myeloma cells.* Int J Cancer, 2013. **133**(6): p. 1357-67.
96. Lin, J., et al., *A clinically relevant in vivo zebrafish model of human multiple myeloma to study preclinical therapeutic efficacy.* Blood, 2016. **128**(2): p. 249-52.
97. Mondanelli, G., et al., *A Relay Pathway between Arginine and Tryptophan Metabolism Confers Immunosuppressive Properties on Dendritic Cells.* Immunity, 2017. **46**(2): p. 233-244.
98. Nguyen-Chi, M., et al., *Identification of polarized macrophage subsets in zebrafish.* Elife, 2015. **4**: p. e07288.
99. Agoro, R., et al., *Cell iron status influences macrophage polarization.* PLoS One, 2018. **13**(5): p. e0196921.